Manuscript title and authors:

Pro-ictal, rather than pre-ictal, brain state marked by global critical slowing and local gamma power increase

I. Dallmer-Zerbe[1,2,*], J. Kopal[1,3*], A. Pidnebesna[1,4], J. Curot[3,5], M. Denuelle[3,5], A. De Barros[6], J.C. Sol[6], L. Valton[3,5], E.J. Barbeau[3,+], J. Hlinka[1,4,+]

Author affiliations:

1 Department of Complex Systems, Institute of Computer Science, Czech Academy of Sciences, Prague, Czech Republic

2 Department of Physiology, Second Faculty of Medicine, Charles University, Prague, Czech Republic

3 Centre de Recherche Cerveau et Cognition (CerCo), Toulouse III University-CNRS UMR 5549, France

4 National Institute of Mental Health, Klecany, Czech Republic

5 Brain electrophysiology, Epilepsy and Sleep Unit, Neurology Department, University Hospital, Toulouse, France

6 NeuroSurgery Department, University Hospital, Toulouse, France

Correspondence to:

[+]Emmanuel Barbeau, Ph.D.

Centre de recherche Cerveau & Cognition (CerCo - UMR5549)

CNRS, Université de Toulouse

CHU Purpan, Pavillon Baudot

31059 Toulouse cedex 9, France

email: emmanuel.barbeau@cnrs.fr

telephone : +33(0)6 223 229 78

[+]Jaroslav Hlinka, Ph.D.

Pod Vodarenskou vezi 271/2

18207, Prague 8

Czech Republic

e-mail: hlinka@cs.cas.cz

telephone: +420 266 05 3808

Key Points:

- We investigated the multi-day changes in brain dynamics during presurgical evaluation of patients with drug-resistant temporal lobe epilepsy, inside the epileptogenic zone as well as in healthy brain tissue.
- This time interval of increasing seizure susceptibility is marked by increases in gamma band power in the epileptogenic zone and network-wide increase in critical slowing.
- The identified multi-day changes were consistently linked to the changes in spikes and high-frequency oscillations (HFOs), while not to other factors like drug dose and circadian time.
- While gamma power and critical slowing changed on the scale of days, there was no significant increase in the minutes before seizures, suggesting the brain dynamic changes during presurgical evaluation are likely a multi-day phenomenon associated with pro-ictal states.

ABSTRACT

The clinical workup during the pre-surgical evaluation for epilepsy relies on the electrophysiological recording of spontaneous seizures. The interval until first seizure occurrence is characterized by an increase in seizure likelihood caused by progressive drug dose decreases, during which the epileptic brain transitions from a state of low to a state of high seizure likelihood, so-called *pro-ictal* state. This study aimed to identify the dynamic brain changes characteristic of this transition from 386 ten-minute segments of intracranial EEG recordings of 29 patients with drug-refractory temporal lobe epilepsy, explored by stereoelectroencephalography, irregularly sampled between electrode implantation and first seizure. As measures of brain dynamics we studied mean phase coherence and relative power in the gamma frequency band, and autocorrelation function width. We further investigate the interaction of those brain dynamics with various susceptibility factors, such as the rate of interictal spikes and high frequency oscillations, circadian and multi-day cycles, and clinical outcomes. We observed a significant increase in relative gamma power in the epileptogenic zone, and an increase in critical slowing in both the epileptogenic zone as well as in presumably healthy cortex. These brain dynamic changes were linked with increases in spike and high frequency oscillations rate. While brain dynamic changes occurred on the slow time scale - from the beginning to the end of the multi-day interval - they did not change in the short-term during the pre-ictal interval. We thus highlight gamma power and critical slowing indices as markers of pro-ictal (as opposed to pre-ictal) brain states, as well as their potential to track the seizure-related brain mechanisms during the presurgical evaluation of epilepsy patients.

INTRODUCTION

Approximately 30% of patients with epilepsy suffer from drug resistance. In these cases, neurosurgery is evaluated as a second-line treatment to remove the brain tissue where the seizure originates. The success of surgery depends on the correct determination of the epileptogenic zone (EZ) and epileptic network. When non-invasive methods (combination of scalp EEG, MRI, PET and neuropsychological assessment) do not identify the EZ, the standard clinical procedure involves the invasive implantation of intracranial (iEEG) electrodes for EZ determination [1,2]. The clinical workup usually includes decreasing drug dosage [3] with the aim to record spontaneous seizures during monitoring. According to literature, it typically takes around two days (median time) until the first spontaneous seizure is recorded [4,5], while 35% of patients require more than three, and 7% require more than a week to record and diagnose the nature of paroxysmal episodes [4]. Understanding these brain processes leading up to the first seizure event could help improve the clinical workup of presurgical evaluation, which is a long and cumbersome procedure; e.g. help to reduce recording length, choose the best time window for stimulation probing, or optimize the drug reduction protocol to avoid withdrawal complications. Furthermore, it could bring fundamental insight into the mechanisms of seizure generation (ictogenesis) in the human brain.

Ictogenesis, as often studied in the context of seizure prediction, is a complex process [6]. It is typically studied on a time scale of minutes up to hours before seizure [7]. In vitro studies have found the time period before seizure occurrence, i.e. the pre-ictal state, to be characterized by a progressive and global increase in neuronal activity, a build-up of low-amplitude high-frequency activity (>100 Hz) and a reduction in system complexity [6]. Immediately before seizure onset, the brain is in a highly sensitive state where even weak perturbations can initiate seizures [6,8]. In vivo studies, on the other hand, have been struggling to reliably map the pre-ictal state [7,9–11]. The complicated nature of the pre-ictal activity, methodological challenges, and the heterogeneity among patients and their seizures have been held accountable [7,9,12,13].

Among the most notable changes observed in iEEG recordings repeatedly linked to ictal transitions is critical slowing down [8,14]. Critical slowing refers to a phenomenon where a system takes longer to recover from small perturbations, indicating an increased risk of transitioning to a different state, such as a seizure. Research has shown that prior to seizures, brain signals may exhibit critical slowing down, which can serve as a warning signal

preceding many critical transitions in dynamical systems [14]. Other notable iEEG changes during ictal transitions as evidenced by several studies are increases in the rate of interictal epileptic discharges, or spikes, and high-frequency oscillations (HFOs > 80 Hz) [15–18], as well as aberrant gamma (30-100 Hz) dynamics prior to seizures. These include changes in gamma power [19,20] and connectivity [21–24]. Such aberrant dynamics are often found within the epileptogenic network [1], and particularly in the EZ [20,23,25]. However, other studies have reported changes outside the epileptogenic network, complementary to those inside [26]. Thus, the ongoing investigation of iEEG biomarkers requires careful consideration of locally specific changes in brain dynamics.

Overcoming the reliability issue of *pre-ictal* markers requires a better understanding of the brain dynamics at play and their influencing factors. Accordingly, epilepsy research has recently shifted its focus from the short-term (and deterministic) prediction of single seizure events to the long-term (and probabilistic) prediction of time intervals of increased seizure risk, searching for so-called *pro-ictal* markers [9,27]. In other words, while *pre-ictal* markers aim to identify the brain changes involved in the immediate seizure transition (typically investigating an interval in minutes before seizure onset), *pro-ictal* markers aim to identify brain changes linked to an increased seizure risk, which have been shown to act on timescales of days, months and even years [28].

When taking into account the slow fluctuations in seizure likelihood over days, months, and years, seizure prediction becomes seizure forecasting [9,29–34]. Examples of common observations in epilepsy linked to these fluctuations are seizure clustering (several seizures occurring close together in time) and the variations in brain responses to the same stimulation at different time points [35–38]. Panagiotopoulou and colleagues [39] identified patient-specific fluctuations in iEEG band power that modulated seizure probability. Similarly suggesting that seizures are modulated by slow dynamics, seizures closer together in time were reported to be more similar [40], and seizures were shown to be influenced by previous seizures [41]. Moreover, a growing body of studies have reported pro-ictal factors that influence seizure likelihood [39,42–44]. The work of Karoly and colleagues [43] demonstrated that seizure occurrence, phase-aligned with patient-specific sleep-and-wave cycles, was linked with changes in the interictal discharge rate. Furthermore, drug dose, weather, and temporal factors (time of day, day of week, and lunar phase) were linked to the slow dynamics in seizure likelihood [42,44–46]. However, the complex link between the epileptic brain processes and such susceptibility factors, remains insufficiently understood. Studying their relationship

can help to answer the fundamental questions of what constitutes *pre-* and *pro-ictal* states in the human brain.

Combining tools from seizure prediction and forecasting, this study aimed to investigate the multi-day pre-seizure mechanisms during pre-surgical evaluation. We hypothesized there would be a progressive *pro-ictal, long-term* increase of seizure susceptibility in this interval linked with drug dosage decreases and other established susceptibility factors. Furthermore, we hypothesized a *pre-ictal, short-term* change in brain dynamics immediately before seizure, linked with seizure initiation. To investigate the pro- and pre-ictal iEEG dynamics, we leveraged three *measures* from the literature in the field of seizure prediction: one for gamma power alterations, the gamma power ratio (gPR) [39], one for gamma synchronization, the mean phase coherence in the gamma band (gMPC) [22,47], and one for critical slowing, the autocorrelation function width (ACFW) [14]. Furthermore, we studied their interaction with several pro-ictal *factors* from the field of seizure forecasting: linear time (time since first recording), daytime, drug dosage, as well as spike and high frequency oscillation (HFO) rate in the frequency range from 80-126 Hz (combined with spikes for higher predictive power [48]). Finally, we added the factor signal-to-noise ratio (SNR) as a control variable to assess data quality, such that low SNR means a high amount of noise in the data. We compared pre-seizure dynamics between the EZ and healthy brain areas in the long- and short-term, i.e., investigating the measures' changes firstly from the beginning of the recording to immediately before the seizure (multi-day changes), and secondly within the last minutes before the seizure (short-term changes).

METHODS

iEEG Data acquisition

Our dataset consisted of intracranial EEG data recorded for 29 patients with drug-resistant epilepsy (Table 1). The patients were monitored at the Brain electrophysiology, Epilepsy and Sleep Unit, department of Neurology, at Toulouse University Hospital to identify and possibly resect the brain areas involved in seizure generation, between 2009 and 2020. If surgery was offered, its outcome was rated using the International League Against Epilepsy (ILAE) rating scale [49]. iEEG were retrospectively collected with the following inclusion criteria: over 12 years of age, temporal involvement in the epileptogenic network, recording electrodes implanted in the temporal lobe, and an available iEEG recording of the

last 10 min before the first recorded seizure. Each patient received detailed information about the objectives of the SEEG technique before intracerebral electrode implantation. Data were collected using the computerized patient records of the Toulouse University Hospital IT system. This data collection was authorized in accordance with the French Data Protection Authority MR-004 reference methodology. Following assessment and validation by the Data Protection Officer and in compliance with general data protection regulations, the research, named Predire (as in Seizure Prediction), is registered in the official retrospective studies register of the Toulouse University Hospital, managed by the Research and Innovation Department (RnIPH 2020-130), and is covered by the MR-004 law (CNIL number: 22.6723 v 0). The ethical conditions of this study have been upheld and approved by the Toulouse University Hospital. Consent was obtained from all patients. The implantation was individually tailored to the hypotheses of EZ according to a noninvasive assessment, and the placement of each depth electrode was based exclusively on clinical criteria independently of this study. Standard intracranial electrodes (Microdeep depth electrode, DIXI medical, France) with 8-15 platinum/iridium contacts (diameter 0.8 mm, contact length 2 mm) were used. Intracranial EEG activity was recorded using two synchronized 64-channel acquisition systems (SystemPlus Evolution, SD LTM 64 EXgPRESS, Micromed, France) with varying sampling frequencies (at least 256 Hz) and high pass-filtered to 0.008 or 0.15 Hz. An example recording is given in Fig. 1A. Electrode placement across all patients covered a wide-spread brain network (Fig. 1B).

The iEEG recording started in the hours after electrode implantation and lasted the whole hospital stay. Due to storage limitations, the hospital did not keep all iEEG recordings. This study focused on the interval between implantation and first seizure, which was of variable length across patients (Fig. 1C). Furthermore, we only considered recordings from 10 a.m. the day after the surgical procedure in order to avoid the influence of anesthetics on the measured brain activity. If the interval between the first considered recording and first spontaneous seizure was less than a day, the patients were not considered for the long-term analysis (n = 19), but only the short-term analysis (n = 29; analyses described below). The number of resulting iEEG segments in the chosen interval varied among patients (Fig. 1D; mean = 13, std = 16 across all 29 patients; mean = 20, std = 16 across the 19 patients of the long-term analysis). The time points of recordings were scattered across the chosen interval (Fig. 1E), leaving gaps of up to a couple of days in between them (e.g., sub-08 in Fig. 1E).

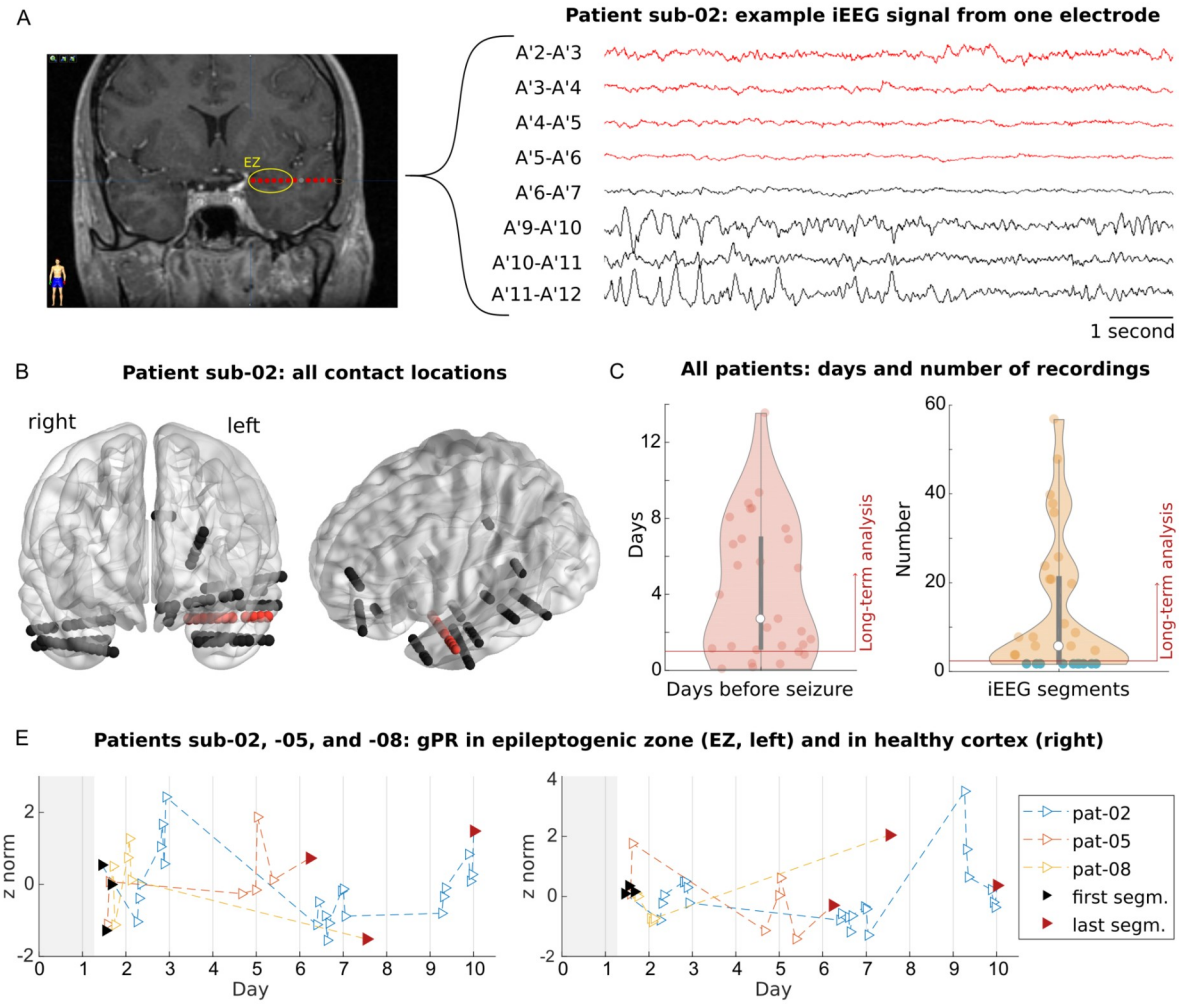

Figure 1

Data description and study design. A: *Example iEEG of recording during interictal phase. The MRI scan on the left side shows an intracranial electrode targeting the left hippocampus in sub-02. Electrodes channels (macro contacts) in the epileptogenic zone (EZ) are highlighted in red. Schematic representation on the right side depicts example signals from the eight bipolar channels. Red traces correspond to bipolar channels located in EZ* ***B:*** *Locations of all bipolar channels for the selected patient referenced in the MNI space (BrainNet Viewer). The intracranial electrode targeting the left hippocampus is marked in red,* ***C:*** *Number of days between electrode implantation and the occurrence of first seizure. Only patients with more than one day of recordings between the implantation (10 a.m. the second day after the procedure) and first seizure were included in the long-term analysis (red line). All patients were included in the short-term analysis (analyses described in Methods).* ***D:*** *Number of available recordings. The number of analyzed iEEG segments varied (mean = 13, std = 16) across the 29 participants. In the short-term analysis, only a single recording (in turquoise) was used per patient.* ***E:*** *Study setup exemplified in three patients: sub-02, sub-05, and sub-08 (see Table 1). Patients had different numbers of segments available (triangles), variably*

scattered across the interval between the day of their implantation (day 0) and the day of the seizure (here, day 6, 7 and 10). Recordings before 10 a.m. on day 1 were excluded to avoid the immediate effects of implantation (interval marked in gray). Mean measure (here gamma power ratio gPR) across time and channels in each recording was compared between different brain areas (left vs. right panel). Long-term changes were assessed by comparing only the first and the last recorded segment (black and red triangles). Short-term changes were assessed within the last recorded segment (red triangle).

Data processing

All processing of iEEG data was conducted with Matlab (Version 9.8.0, The Mathworks Inc, Natick, MA, USA) and the interactive Matlab toolbox EEGLAB [50]. For each patient, we collected all available iEEG recordings before the occurrence of a first seizure (Fig. 1E). For each recording, we then extracted one 10-minute segment for every hour. As an example, an iEEG recording that was three-hour-long would be segmented into three segments. Further preprocessing steps were applied to all iEEG segments. These steps included downsampling to 256 Hz, high-pass filtering with a cut-off frequency of 0.5 Hz, removing non-EEG channels, re-referencing to bipolar montage (single bipolar montage is referred to as a “channel" throughout this study), and finally, the exclusion of error channels. For re-referencing, the difference in activity between (only) directly neighboring channels was calculated. Error channel rejection consisted of a two-step procedure using EEGLAB *pop_rejchan()* function with the `spec' rejection method. Firstly, channels with significantly high power in the 48-52 Hz frequency range (>3 standard deviations from mean channel power in this range), and secondly, outlier channels with regards to the whole 1-128 Hz frequency range (>4 standard deviations from mean channel power) were identified. To obtain a consistent number of channels for each patient across all respective recordings, the same error channels (accumulated error channels over all segments) were excluded from all segments for a given patient. For the same reason, iEEG channels that were present in some but not all segments were disregarded.

Mapping brain dynamics

The aim of the presented study was to map the multi-day pre-seizure dynamics during presurgical evaluation. To explore the brain dynamics preceding the first spontaneous

seizure, we studied the temporal evolution of brain behavior using measures of critical slowing, altered synchrony and altered gamma power (30-100 Hz) in all patients. Specifically, we calculated gamma power ratio (gPR; Fig. 1E), mean phase coherence in gamma band (gMPC), and autocorrelation function width (ACFW). To obtain robust measure estimates over the whole 10 min iEEG segment, we calculated the respective measures in 10 consecutive windows of 60 seconds lengths and averaged them across all windows. This approach was based on exploratory results of measuring stability in a 2 hours long segment (Sup. Fig. 1).

Power ratio in the gamma frequency band (gPR):

In order to provide insights into the dynamics behind neuronal synchronization, we estimated the power ratio in the gamma frequency band using Welch's power spectral density algorithm for every 60s segment of the iEEG recording [39]. Specifically, we computed power spectral density using a sliding window of 500 ms length and a shift of 16 ms. Each sliding window was multiplied by a Hanning window to smoothly taper the endpoints to zero and mitigate the discontinuity that produces leakage. The modified periodograms were averaged to obtain frequency-resolved power spectral density estimates for the 60s iEEG segment. Then, the vector of frequency-varying power spectral density estimates was log-transformed and subsequently Sigmoid transformed ($S(x)=1\left[1+\exp(-x)\right]^{-1}$) to ensure positive entries between 0 and 1 as in previous research on iEEG [39]. As the last preprocessing step, we averaged (across segments) the preprocessed estimates for each of the five main frequency bands: δ: 1–4 Hz, θ: 4–8 Hz, α: 8–13 Hz, β: 13–30 Hz and γ: 30–100 Hz. Finally, the power spectral density estimate in the gamma band was normalized by the average power spectral density in all other bands to obtain the power ratio in the gamma frequency band.

Mean Phase Coherence in the gamma band (gMPC):

Coherence is a mathematical method quantifying the (frequency-specific) consistency of the relation between two signals representing the activity of two brain regions in our analyses. Mean Phase Coherence (MPC) is an implementation analogue to the established phase locking value, which quantifies frequency-specific phase synchronization between two neuro-electric signals [51]. MPC, has been proposed by Mormann and colleagues [22] as a measure of the phase synchronization in EEG recordings of epileptic patients.

In this study, we used an implementation of MPC from Bruña and colleagues [47], where the MPC is calculated as

$$MPC_{i,j} = \frac{1}{T}\left|\sum_{t=1}^{T} e^{-i\left(\varphi_i(t)-\varphi_j(t)\right)}\right|,$$

where T is the length of the iEEG signal, φ_i is an instantaneous phase as obtained by Hilbert transform of the iEEG signal and i, j correspond to the pair of channels for which MPC is computed.

For each 60s window, we calculated gamma Mean Phase Coherence (gMPC) between each pair of iEEG channels in the gamma frequency band (30-100 Hz). Therefore, gMPC between all pairs of channels is represented by a matrix of real-valued numbers between 0 and 1.

Critical slowing down: Autocorrelation function width (ACFW):

The change from normal to a seizing state can be viewed as a critical transition happening in the complex dynamical system (i.e., the brain). This system approaching the critical transition can be characterized by critical slowing down features, where the ACFW represents one of the most commonly used measures [14]. The autocorrelation function measures the correlation of the signal with its shifted copy. High autocorrelation for higher lags between the signal and its shifted copy indicates a smooth signal, while white noise, for example, has low autocorrelation for all positive lags. In this study, ACFW was estimated based on the implementation of Maturana and colleagues [14]; as the width at the half maximum of the autocorrelation function. An increase in this measure would indicate a broadening of the autocorrelation function and thus a slowing of the observed dynamics, which might indicate that the system approaches the critical transition (seizure).

Susceptibility factors

We further explore the relationship of estimated brain dynamics measures with other *factors* that could potentially explain changes in brain dynamics. Namely, we quantified the influence of administered drug dose, elapsed time from electrode implantation, time of the day, signal-to-noise ratio of iEEG recordings, as well as spikes and high-frequency oscillations present in the recordings. For each of these five *factors*, we derived a single metric to characterize the 10-minute iEEG segment.

Drug dose:

The factor of drug dose can be reflective of a patient's seizure susceptibility. The anti-seizure medication was slowly decreased from the first day of recordings to facilitate seizure occurrence. We performed a normalization of administered drug doses since a different dose and different drugs were prescribed to each patient. First, for each administered drug, we normalized the actual dose by dividing it by the maximal dose administered in the interval from admission to first seizure. Then, dosage at a defined time point corresponded to the mean of relative drug dose averaged across all drugs pertinent to the most recent drug administration (e.g. drugs administered at 6 p.m. combined into one score served as an estimate of current medication level for the duration until next drug administration at 9 p.m.). Since the calculated summary index ranges between 0 and 1, it is comparable across patients. In this mapping, the highest relative dosage (i.e., 1) corresponds to the lowest susceptibility to having a seizure.

Linear Time:

Seizure susceptibility was reported to fluctuate over daily timescales [40]. We thus characterized each iEEG segment by the time elapsed from the iEEG electrode implantation.

Daytime:

Prior research shows that circadian timescales influence seizure susceptibility [52]. To take into consideration the influence of the time of the day (i.e., day and night cycles) on the estimated measure of brain dynamics, we characterized each iEEG recording by daytime at the beginning of the recording, in 24-hour format (i.e. 14:02:35).

Spikes and high-frequency oscillations (HFOs):

Spikes and HFOs were proven to be valuable biomarkers of epileptogenic tissues. In particular, the combination of both, i.e., the cross-rate, was shown to have superior prediction performance compared to individual measures [53]. We used the AnyWave: Delphos software [54] to detect spikes and HFO (80-126 Hz; maximum frequency limited by the 256 Hz sampling frequency) in each 10 min iEEG segment separately for each channel.

Each channel was then characterized by the cross rate:

$$cross\,rate = \sqrt{spike\,rate * HFO\,rate},$$

where spike rate corresponds to a per-minute estimate of the number of spikes in a given channel (identically for HFO rate). We used mean cross rate across all channels to represent the amount of spikes and HFOs present in a single recording [53].

Signal-to-Noise-Ratio:

As the last factor we quantified the signal-to-noise ratio (SNR). We use SNR as a control assessment that quantifies the clarity and strength of the neural activity. We quantified SNR in each iEEG segment for each channel separately. The used *snr()* function from Matlab's Signal processing toolbox returns the signal-to-noise of the input iEEG signal by comparing the power of the signal estimated from power spectral density to the power of the noise. SNR is estimated across the entire frequency spectrum of the signal, providing a comprehensive assessment of signal quality. The resulting SNR value is in decibels (dB).

Description of the data analyses

Long-term changes, first-to-last:

In order to assess long-term changes in brain dynamics, we compared the "first" iEEG recording segment after 10 a.m. the day after electrode implantation (to avoid immediate effects of the implantation procedure, such as effects of narcosis medication) with the "last" iEEG recording segment right before the seizure. Specifically, we compared the measures characterizing the first segment to the measures of the last segment using the Wilcoxon signed-rank test. Subsequently, we tested whether the change (Last - First) in EZ was greater than the change in healthy cortex (defined as channels remaining unlabeled by clinicians; thus excluding also other zones, such as irritative and lesion zones) using Wilcoxon signed rank test at 0.05 significance level (i.e., Change in EZ - Change in healthy cortex > 0). All resulting p-values were FDR-corrected using the Benjamini/Hochberg procedure across the three measures (and the two zones for the first comparison).

In a post-hoc exploration, we quantified the linear association strength of the measure changes with changes in the *factors* and continuous clinical variables (age, time since epilepsy diagnosis at the time of hospitalization, and the number of electrodes in EZ) using

Pearson's correlation. Finally, we used a two-sample t-test to examine the relationship between measure change and binary clinical variables (sex, hemisphere of EZ, resection hemisphere, surgery outcome), at 0.05 significance level.

Long-term changes, dissimilarity:

The following pipeline aimed to investigate the evolution of brain dynamics in all available iEEG recordings separately for each patient. Due to the irregular sampling of the recordings, we here adopted the methodology from Schroeder and colleagues [40]. Specifically, we quantified the dissimilarities in brain dynamics between all pairs of iEEG recordings.

Based on the above-described procedure, each patient was described by the brain dynamics *measures* in each iEEG channel computed over the 10-minute segments. These measures were in the form of vectors for gPR and ACFW (dimensions: number of channels × 1) and matrix for gMPC (dimensions: number of channels × number of channels). Therefore, for gMPC, we first vectorized the connectivity matrices by taking the upper triangular vector without the diagonal. In doing so, each iEEG segment was represented by a single brain dynamics vector. The ensuing brain dynamics dissimilarities were defined as the mean L1 distance between two brain dynamics vectors.

To be able to compare the dissimilarity of brain dynamics with our five *factors*, we also calculated factor dissimilarity. The dissimilarities of linear time and daytime were based on the time elapsed between the respective times of each two measurements. The drug dose dissimilarity was calculated as the absolute difference between two drug doses. The dissimilarity in spike and HFO profiles between the two measurements was based on a correlation between their respective cross-rates (rates across channels):

$$CR_{dissimilarity} = \frac{1 - r_{i,j}}{2}$$

where $r_{i,j}$ represents Pearson correlation between the cross-rate of segment i and j.

An identical procedure was applied to signal-to-noise ratio dissimilarities.

Finally, we quantified the relationship between brain dynamics dissimilarities and factor dissimilarities. We computed Spearman's correlation between the upper triangular elements of the brain dynamics dissimilarity matrix and each factor matrix.

Short-term changes, trend analysis:

The examination of short-term changes was based on the analysis of *trends* which are represented by the correlation of the minute-resolved measures (gPR, gMPC, ACFW) with time. We tested whether the *trends* in EZ are higher than those in healthy cortex using the Wilcoxon signed rank test across patients, at 0.05 significance level.

RESULTS

iEEG dataset and patients' characteristics

We studied multi-day intracranial EEG data from 29 patients with drug-resistant, temporal lobe epilepsy (see Table 1: Patient Characteristics). The patients mean age was 33 ± 13 (range: 12 to 58) years and mean epilepsy duration was 18 ± 12 (range: 4 to 50) years. The patient sample comprised 19 males and 10 females. Patients had on average 12 ± 2 (range: 7 to 16) implanted electrodes and 116 ± 13 (range: 83 to 127) recording channels. Out of those, EZ, as identified by the clinicians during monitoring, included on average 13 ± 12 (range: 2 to 61) channels, which were localized in the left hemisphere in 16, right in 10 and in both hemispheres in three patients. Surgery was later conducted in 19 of the patients, achieving seizure freedom in 12 patients (ILAE score 1) one year or more after surgery and improvement despite remaining seizures in 4 patients (ILAE score 2-4 [49]).

Long-term, pro-ictal changes between electrode implantation and first seizure

In the first part of the analysis, we investigated long-term changes in gPR, gMPC, and ACFW brain measures that could indicate a slow build-up in the brain mechanisms leading up to the first seizure during the interval of pre-surgical assessment. To that end, we compared the first iEEG recording segment after electrode implantation with the last iEEG recording segment before the seizure (red and black triangles in Fig. 1E). We included only patients in which this interval was at least one day (n = 19). The change from the first to the last segment was thus computed as the difference: (Last - First), so that a positive change would indicate a long-term increase in the respective brain measure.

Table 1: Patient Characteristics

Patient	MRI lesion(s)	EZ localization*	duration**	sex	electrodes	channels***	channels EZ	outcome****
sub-01	R HS	R temporal	7	M	16	126	22	ILAE 1 (2y)
sub-02	R HS	L amygdala & hippocampus	6	M	12	117	11	ILAE 4 (2y)
sub-03	R HS	R temporal	21	F	14	124	5	ILAE 1 (2y)
sub-04	R HS, sequelae of ganglioma surgery	R temporal	11	F	11	125	12	ILAE 1 (1y)
sub-05	none[a]	L temporal	6	M	11	118	16	ILAE 5 (11y)
sub-06	R HS	R temporopolar	16	M	11	111	35	ILAE 5 (12y)
sub-08	R HS	R temporal	5	M	11	120	6	ILAE 1 (3y)
sub-09	HS	L temporal	38	M	12	88	8	ILAE 3 (3y)
sub-10	bilateral HS	L temporal	19	M	10	117	11	NA
sub-12	L HS	L temporal	10	M	10	117	10	ILAE 1 (4y)
sub-15	L colliculus cyst, L mamillar and fornix atrophy	L frontal	18	M	14	127	2	NA
sub-16	L reactional gliosis, ischemic neuronal lesions	L temporal	32	F	11	114	2	ILAE 5 (9y)
sub-17	R cortical temporal atrophy	bitemporal	50	F	12	120	15	NA
sub-18	bilateral post traumatic sequelae	bitemporal	8	M	13	125	5	NA
sub-20	L HS	L temporal	20	M	13	126	12	ILAE 4 (6y)
sub-21	L temporopolar meningoencephalocelis	L temporal	20	M	12	127	61	NA
sub-22	none	L temporal & L medial	13	M	14	127	4	NA
sub-23	L HS, occipito-temporo-parietal sequelae	L temporal	29	M	10	111	2	NA
sub-24	L HS	L temporal	14	F	11	118	3	ILAE 1 (6y)
sub-25	L HS	L temporal	10	F	13	127	10	ILAE 1 (4y)
sub-26	R HS	R temporal	17	M	9	127	4	ILAE 1 (4y)
sub-27	R HS	R temporal & R orbitofrontal	49	F	12	112	17	NA
sub-28	L HS	L temporal	13	M	11	119	12	ILAE 4 (7y)
sub-30	R HS	R temporal	8	F	7	83	14	ILAE 1 (8y)
sub-31	R hippocampal atrophy, medotemporal & polar hypersignal[b]	L temporal	9	M	13	120	9	NA
sub-32	L cortical frontotemporal atrophy	L insular	25	F	9	83	20	ILAE 1 (4y)
sub-33	sequelae of surgery of plexus choroid carcinoma	R temporal	17	F	9	97	9	ILAE 1 (5y)
sub-34	L hippocampal heterotopia	bitemporal	34	M	14	127	24	NA
sub-35	DNET	R temporal	4	M	11	120	9	ILAE 1 (8y)

*EZ localization after the final medical conclusions at the end of the SEEG; **duration of epilepsy at time of hospitalization; ***channel numbers as available in data recording files; ****surgery outcome – if offered – as assessed at a variable time interval after presurgical evaluation, denoted for each patient in years (y).
[a]reactional gliosis, ischemic neuronal lesions; [b]"neuronal injury associated with neuronal dispersion", ischemic neuronal lesion in amygdala, gliosis in lateral temporal
DNET: Dysembryoplastic Neuroepithelial Tumor; F: female; HS: hippocampal sclerosis; ILAE: International League Against Epilepsy; M: male; MRI: magnetic resonance imaging; NA: not administered

We first investigated whether the measures captured similar brain behavior. Thus, we quantified the relationship (across patients) between the changes of ACFW, gMPC, and gPR. Fig. 2A shows the Spearman correlation between any pair of measures. We did not observe any significant correlation, neither in EZ nor in presumably healthy cortex. This absence of significant association indicates that the measures capture different aspects of brain activity.

We further repeated the same procedure to probe the interdependence of *factors*. Fig. 2B shows the correlation between any pair of *factors*. As one aspect of the clinical procedure is to reduce anti-seizure medication until occurrence of the first seizure, patients with a longer time until first seizure had a higher decrease in drug dose (r = -.800, p < .001). Furthermore, we did not expect spikes and HFO in the healthy cortex except for some false alarms detected by our automatic procedure. In accordance, the rate of spikes and HFOs correlated with the level of SNR in the healthy cortex (r = .647, p = .003). In summary, we confirmed our expectations regarding the interdependence of *factors* and demonstrated the independence of the brain measures under investigation.

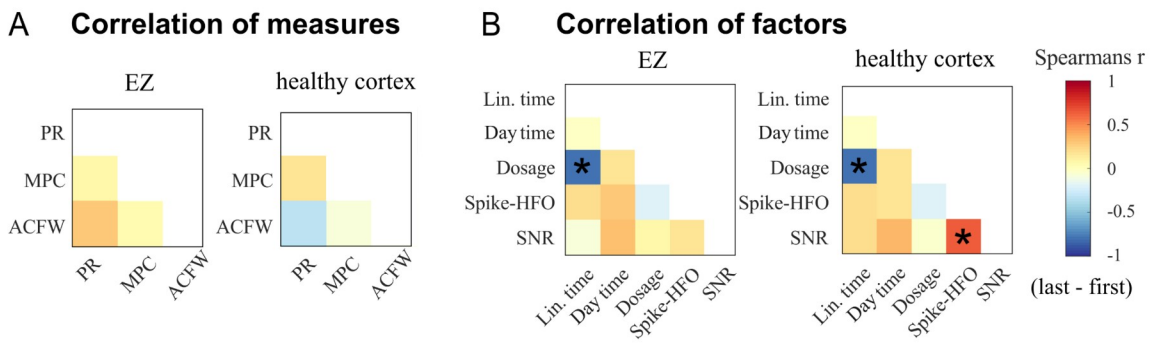

Figure 2

Measure and factor correlations between (Last - First) in EZ and healthy cortex. ***A:*** *The measures did not correlate significantly one with the other, indicating that the measures capture different aspects of brain activity.* ***B****: The factors showed expected correlations of drug dose with time, as well as spikes and HFOs with SNR (noise) in the healthy cortex.*

After establishing the relationships between the measures, we studied the change in ACFW, gMPC and gPR from the first to the last iEEG recording. In line with a slow build-up in the pre-seizure brain dynamics, we expected to find a long-term increase in the measures localized to EZ. For statistical assessment, we tested for such an increase in EZ compared to the change in the healthy cortex separately for the three measures (FDR corrected to control for multiple comparisons). We found that most patients showed an increase of gPR, i.e, relative gamma power, in EZ but not in the healthy cortex (Fig. 3A, left panel). Accordingly, across patients there was a significant localized increase in gPR (one-sided, Wilcoxon signed rank test of Change in EZ - Change in CTRL > 0; $Z = 2.515$, $p_{FDR} = .033$, Cohen's $d = .678$). The change in gMPC, i.e. gamma synchrony, while pointing into the expected direction (Fig. 3A, middle panel), did not reach the significance level after FDR correction ($Z = 1.912$, $p_{FDR} = .077$, $d = .258$). These results did not change when removing the two outlier patients. Finally, for ACFW (Fig. 3A, right panel), i.e. critical slowing, we did not find the expected localized increase in EZ as compared to CTRL ($Z = -0.584$, $p_{FDR} = .720$, $d = -.300$). However, instead of a localized increase, we found a network-wide increase in ACFW with significant increases in both healthy cortex ($Z = -2.757$, $p_{FDR} = .009$, $d = -.680$) and EZ ($Z = -1.992$, $p_{FDR} = .046$, $d = -.545$), when tested separately. In summary, we found indications of a long-term build-up in pre-seizure brain dynamics during presurgical evaluation as captured by a localized increase of gamma power, but not synchrony, in EZ and a network-wide increase of the critical slowing index.

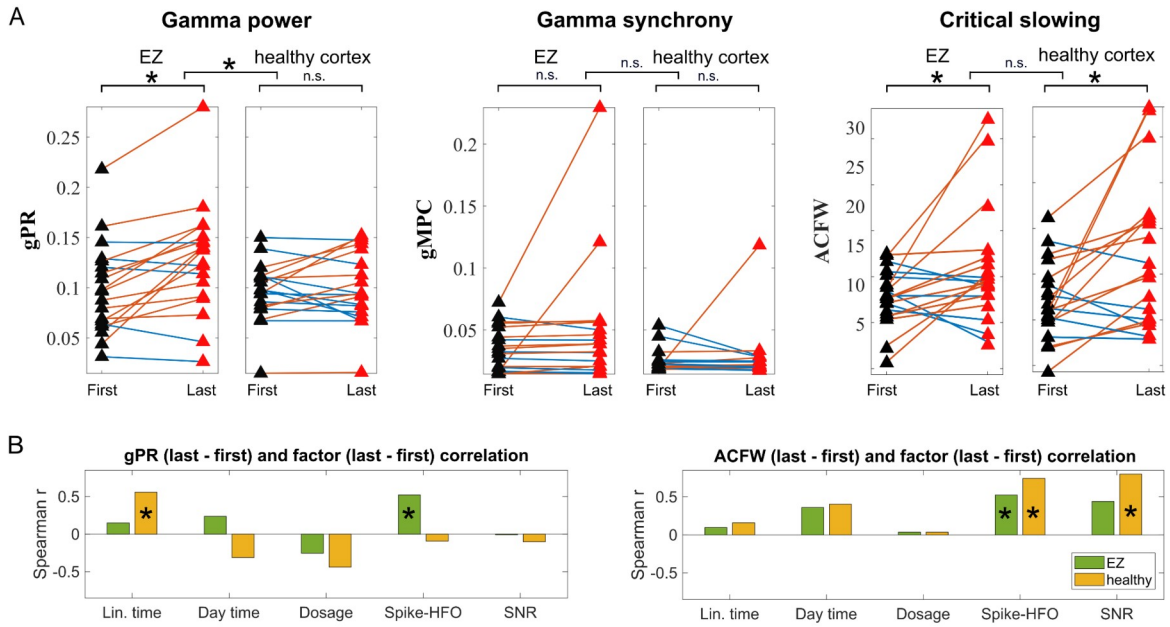

Figure 3

Long-term changes between the first and last segment. A: *Changes of measures in EZ vs. healthy cortex for all patients. Relative gamma power (gPR: 30-100 Hz) in EZ of most patients displays an increase (red lines) as opposed to a decrease (blue lines). Mean phase coherence (gMPC) change did not reach significance after FDR correction. Changes of autocorrelation function width (ACFW) are observed both in EZ and healthy cortex.* ***B:*** *Post-hoc analysis of gPR and ACFW change: correlation of first-to-last changes with the changes in factors. The gPR increase in EZ was accompanied by an increase in Spike and HFO rates. The ACFW increase in both healthy cortex and EZ was accompanied by an increase in Spike and HFO rates. n.s.: not significant; SNR: signal-to-noise ratio.* * *represents* $p < 0.05$.

In a post-hoc exploration, we searched for the association between the gPR and ACFW increases and changes in the *factors* (Fig. 3B). In EZ the increase in gPR was significantly positively correlated with changes in spike and HFO rate (Spearman's $r = .521$, $p = .022$). Thus, changes in gamma power in EZ from the beginning of a patient's recording until immediately before their first seizure were associated with changes in spikes and HFOs. In the healthy cortex, as expected, we found no such relationship between gPR increase and spikes and HFOs. Similarly, the network-wide ACFW increase was accompanied by an increase in spikes and HFOs, both in the healthy cortex ($r = .744$, $p = .000$) and EZ ($r = .523$, $p = .023$). Thus, spikes and HFOs were consistently linked to the multi-day changes of brain dynamics during the multi-day pre-seizure interval. Other factors were less consistently

linked. Notably, we did not find a significant relationship between the observed changes in brain dynamics and the time it took until seizure occurred or the changes in administered drug dose.

Finally, as a sensitivity analysis, we probed whether the identified gPR and ACFW increases were associated with clinical variables (Sup. Fig. 2). Specifically, we tested the linear relationship between the measure increase with age and time since epilepsy diagnosis at the time of hospitalization ('duration' in Table 1: Patient Characteristics). We further tested for a group difference in the gPR increase based on sex (male vs. female), hemisphere of EZ and resection (left vs. right), and surgery outcome (ILAE 1 vs. ILAE 3-5). We did not find any significant association or difference between any clinical variable and the measure increases. Thus, the gamma power and autocorrelation increases can be interpreted as rather general phenomena in the context of (drug-resistant) temporal lobe epilepsy.

Pro-ictal brain dynamics are related with factor dynamics

In the next step of our analysis, we aimed to study the long-term dynamics of the observed changes in brain dynamics using all available iEEG recordings (compared to the above analysis of First and Last recordings only; see Fig. 1). To that end, we conducted a dissimilarity analysis between all pairs of iEEG segments extracted from all the available recording time points. We expected a gradual increase in gPR and ACFW during the whole time interval, indicated by a positive correlation between the temporal distance of two data segments and their observed gPR difference. In addition, we speculated that pairs of segments recorded at a similar time of the day, a similar drug dose administered, or with a similar amount of spikes and HFOs would have more similar gPR, indicating a relationship between long-term pre-seizure brain dynamics and the *factors*.

In this long-term analysis, for each patient with at least a day between the first segment and first seizure occurrence (n = 19), we compared each available segment with all other segments, separately for the *measures* that had shown significant results in the previous analysis (gPR and ACFW) and the *factors* (linear time, daytime, drug dose, spike and HFO rate, SNR). In doing so, we obtained one dissimilarity matrix for each measure as well as for each factor per patient (Figure 4A, *top*). Within a given patient, we then correlated the dissimilarity matrices of gPR with those of the factors, resulting in one correlation value for each factor (Figure 4A, *bottom*).

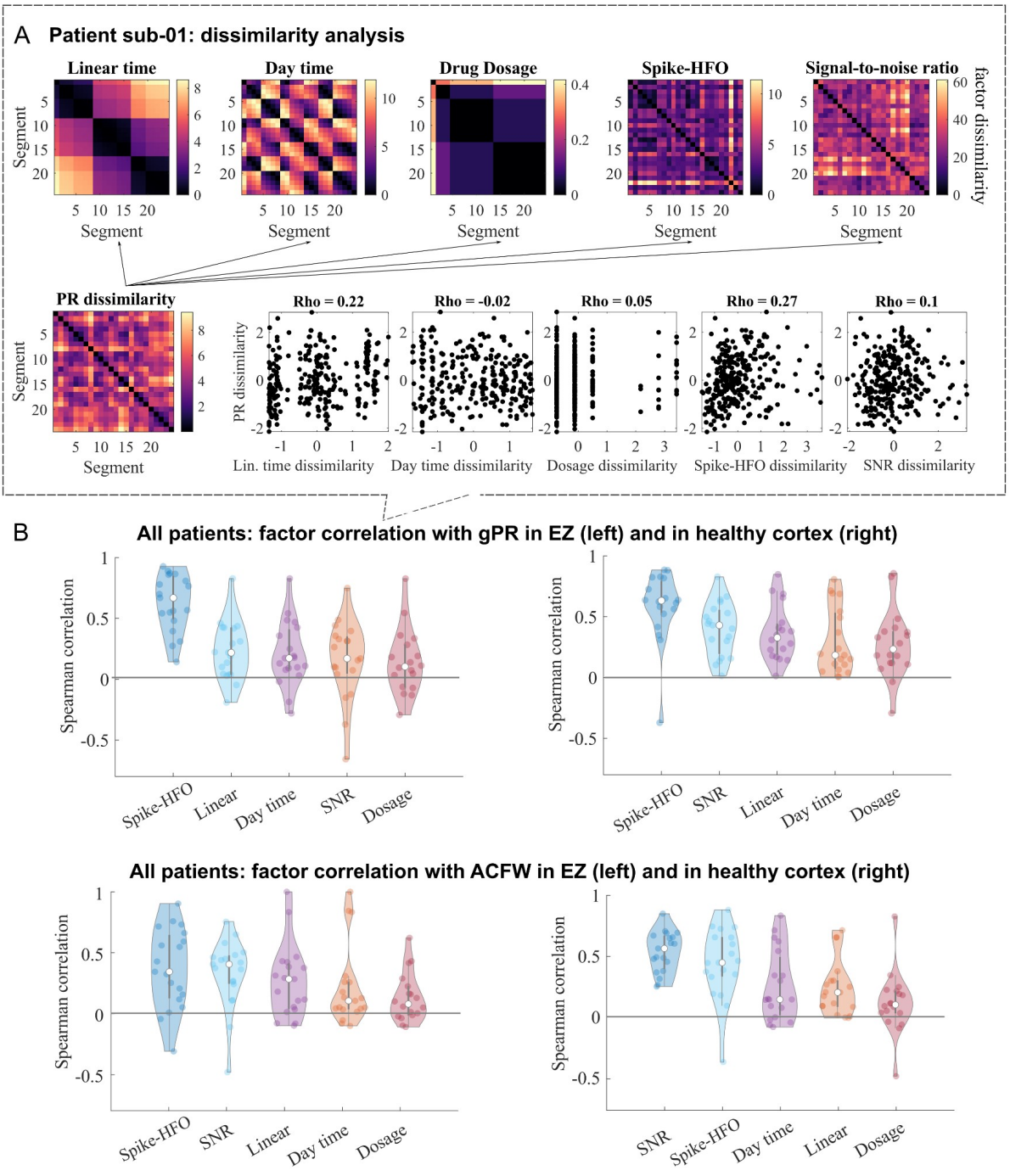

Figure 4

Dissimilarity analysis of factor correlations and the relationship of gPR with spikes and HFOs across patients and zones. ***A****: Dissimilarity in factors (top row) and gPR (bottom left) between all pairs of data segments in exemplary patient Sub-01. For each patient, we then compared the dissimilarity of gPR and factors using Spearman's rho. Therefore, we obtained a single correlation value for each pair of recordings (bottom right).* ***B****: Correlation results for the different factors across patients in EZ and in the healthy cortex. Overall, the relationship between the dissimilarity of measures (gPR and ACFW) and factors (SNR, Spikes, Day time, Linear time, Drug dosage). All*

factors correlated on average above zero. Among the different factors, spikes and HFO rate were most consistently linked to measure changes. Surprisingly, drug dosage had the lowest similarity with measure changes. Spikes in the healthy cortex are most likely due to false detections of the automatic spike detection procedure.

Based on the comparison of factor-specific correlation coefficients across patients, we observed similar factor interactions for EZ and healthy cortex (Figure 4B). On average, the dissimilarity of each factor correlated positively with the dissimilarity of gPR. In other words, across patients, pairs of segments that were more similar in their factor value (e.g. closer in time) were also more similar in gPR. Among the different factors, spikes and HFO rate showed the strongest link, while drug dosage showed the lowest similarity on average. On a patient level, the correlation coefficients varied (e.g. correlation of drug dose dissimilarity and gPR dissimilarity in EZ from r = -0.293 to r = 0.828). Thus, while in some patients, there were very strong indications of a gradual build up in pre-seizure brain dynamics, circadian time- and/or drug-dose dependence, in others, such indications were weaker. Overall, the dissimilarity analysis confirmed the findings of the first-to-last comparison: spikes and HFOs showed a consistently strong relationship with the changes in the measured brain dynamics, while drug dosage and other factors did not.

Studying the spike and HFO rate dynamics individually, we observe both increases and decreases across the long-term interval between implantation and the first seizure (Fig. 5). Thus, the link between brain measures and spike and HFO rate dynamics (compare Fig. 1E and Fig. 5A) is more complex than simultaneous increases during the multi-day interval.

Short-term, pre-ictal changes in brain dynamics minutes prior to seizure

In the last step of the analysis, we focused on brain dynamics in the immediate time window around the onset of the first seizure (Fig. 2) that would be indicative of the incoming seizure (Fig. 6). Specifically, we investigated whether there was a short-term increase in the brain measures within the last 10 minutes preceding seizure onset (i.e., in the Last segment). Therefore, we computed the three measures (gPR, gMPC, ACFW) for every minute of the last segment. We then correlated the resulting measure values with time. These correlation coefficients we call *trends*. Positive *trends* indicate a linear increase in the measure before seizure onset, while negative *trends* indicate a linear decrease over time.

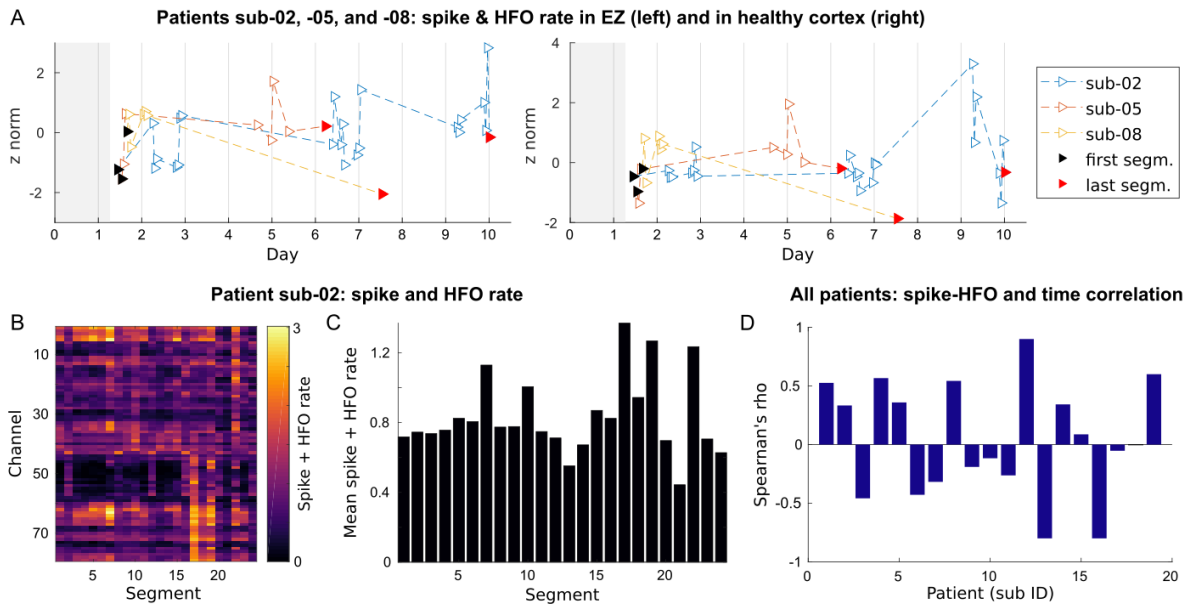

Figure 5

Spike and HFO characteristics in long-term analysis. ***A:*** *Spike and HFO rates exemplified in three patients: sub-02, sub-05, and sub-08 (see Table 1). Each iEEG segment (triangle) was characterized by a summary of spikes and HFO: a cross-rate.* ***B:*** *Spike and HFO rate in an exemplary patient (sub-02). We estimated the amount of spike and HFO rate in each channel and each segment.* ***C:*** *Average spike and HFO rate. The estimated rates were averaged across channels to provide an estimate for each segment.* ***D:*** *Linear trend in spike and HFO rates. Finally, we correlated the segment-specific spike and HFO rates with the times of respective measurements. The resulting correlation varied significantly, suggesting that both increase and decrease in the spike and HFO rates are observable across patients as we approach the seizure.*

Within an additional exploratory analysis, in all measures and especially gPR, we observed larger variance (measured in standard deviation) across patients prior to seizure in EZ as compared to healthy cortex (Fig. 6A). In the first minute after seizure onset, gPR and gMPC typically increased, and ACFW decreased in EZ. The changes in these measures after seizure onset were also present in the healthy cortex; however, they were typically less pronounced and occurred later. These observations highlight the disparity between detecting markers of upcoming seizures and detecting the impact on brain dynamics of the seizure itself.

In line with the long-term results, we probed for a linear association between the short-term *trends* in the measures with spikes and HFOs. Same as for the measures, the *trend*

in spikes and HFOs was computed via correlation of minute-wise change in the last 10 minutes before seizure with time. The short-term gPR *trends* significantly correlated with spike and HFO *trends* across patients. Notably, we observed the same relationship in the long-term analysis. This factor association was observed in EZ but not in the healthy cortex (Fig. 6B), supporting the role of epileptic spikes and HFOs in pre-seizure gamma power increases, both in the long- and short-term.

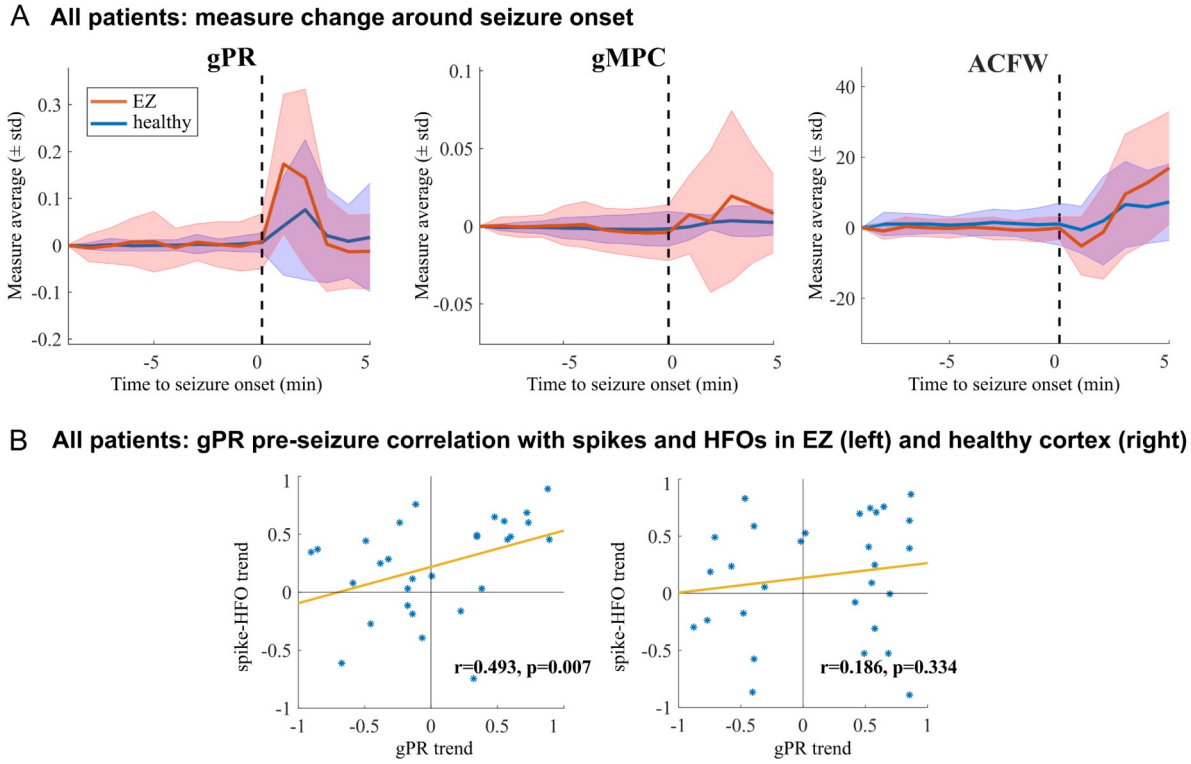

Figure 6

Short-term changes around seizure onset. *A: Measure mean and standard deviation before and after the onset of the seizure (dashed line). After seizure onset, gPR and gMPC showed an overall increase, while ACFW displayed a decrease in EZ. Measure changes around the seizure onset in the healthy cortex were weaker compared to EZ. The solid line depicts the mean measure across all patients. The shaded area represents the standard deviation of the given measure. B: Relationship between measure trend and HFO trend. Short-term trends in gPR are related to Spikes and HFO in EZ but not in the healthy cortex.*

DISCUSSION

This study investigated multi-day changes in brain dynamics during the presurgical evaluation of epilepsy patients; more specifically, the time interval between electrode implantation and the occurrence of the first spontaneous seizure. We find long-term increases in gamma band power prominent in the EZ and a network-wide increase in critical slowing from the beginning to the end of the interval (Fig. 3). We found no significant changes in gMPC (short- or long-term), but a potential long-term change could have failed significance testing due to the limited sample size. The identified long-term changes in gPR and ACFW were consistently linked to the long-term changes in number of spikes and HFOs detected. This link was further supported by a dissimilarity analysis (see Fig. 4), exploring the pairwise relationship between all extracted 10 minute segments of iEEG data scattered across the multi-day interval. Other *factors*, such as drug dose and circadian time did not show a consistent relationship with the identified brain changes. Investigating the long-term spike and HFO dynamics (Fig. 5), we find both patient-specific in- and decreases. Finally, while gamma power and critical slowing changed on the time scale of days, they did not show a significant increase in the minutes before seizure (Fig. 6), indicating that the brain dynamic changes during presurgical evaluation could in fact be a multi-day phenomenon with changes occurring on a slow time scale.

The novelty of this study was to investigate iEEG changes in the interval leading up to the first seizure during presurgical monitoring - a time window presumably marked by a progressive increase in seizure likelihood. We studied different time scales (multi-day vs. minutes before seizure), network locations (EZ vs. healthy cortex) and the interaction with several pro-ictal factors, previously linked to the seizure-modulating processes [39,42–46].

Concerning time scales, we observed the changes in gPR and ACFW measures during the multi-day interval only, but not in the last minutes before seizure. The observed long-term increase in gPR and ACFW found in this study confirms previous findings on gamma power increases and critical slowing prior to seizures [14,19,20,55]. They support and extend the findings of Maturana and colleagues [14], who showed that seizures align with the increasing phase of ACFW on a slow time scale. Moreover, slow fluctuations in iEEG power as described in Panagiotopoulou and colleagues [56] could be linked to the multi-day gPR changes identified in this study, but not to circadian fluctuations as we did not find consistent correlations with the factor of daytime. We interpret the absence of a short-term increase pre seizure in these measures such that the observed changes capture pro-ictal brain states (during an increased

seizure likelihood), as opposed to pre-ictal states (during a single seizure transition; see detailed discussion below).

For network locations, gPR increased locally in EZ (same as in [20]). Aberrant dynamics in epilepsy are commonly found within the epileptogenic network [1]. However, other studies have reported changes outside the epileptogenic network, complementary to those inside [26]. Unlike in Naftulin and colleagues [26] we did not see indications of a systematic decrease in gamma power outside of the epileptogenic network (healthy cortex, see Fig. 3). ACFW on the other hand showed a network-wide increase, supporting Maturana and colleagues's hypothesis, that critical slowing characterizes a state change throughout the whole brain, rather than in a localized brain region [57].

For the studied pro-ictal factors, spikes and HFOs, considered hallmarks of epilepsy [58], showed a consistently significant link to the multi-day changes in autocorrelation and critical slowing. Other factors, including linear, circadian time and drug dose did not show a consistent link with the observed measure changes in this study. The relationship between pre-ictal brain dynamics and spikes and HFOs was previously established [15–17,59], especially between spikes and HFOs and the changes in high-frequency spectral power [56] and the measures of critical slowing [57]. Importantly, gamma power changes remain after removing spikes from the iEEG signal via signal processing [60]. Thus, spikes and HFOs and gamma power can be assumed to capture complementary signal characteristics. It is important to note that, in our study, the maximum frequency of HFO assessment was limited to 126 Hz due to the sampling frequency of the data, and that there was a partial overlap of the frequency ranges of the two (gPR: 30-100 Hz; HFOs: 80-126 Hz).

A major limitation to this study was the irregular data sampling in the chosen time interval that did not allow us to statistically investigate the multi-day progression of brain measure and factor changes. A continuous dataset is needed to allow the study of the detailed progression of brain states during this interval of presurgical evaluation. However, our results support the potential usefulness of those measures to serve as markers of seizure-modulating processes [39,57]. An advantage of the measures used in this study is that they are easy to apply and computationally inexpensive and thus bear a potential for a clinical translation in the context of tracking epileptic states in epilepsy.

Pro-ictal brain states and the origin of long-term fluctuations in seizure susceptibility

The reliability issues in seizure prediction have recently led to the emergence of the field of seizure forecasting [9,27], and the distinction of a so-called *pro-ictal* brain state, suggested by several recent studies evidencing the existence of time windows of an increased seizure risk and slow fluctuations in seizure susceptibility over time (see Baud et al. for a recent review [28]). Examples of common observations in epilepsy linked to these fluctuations are seizure clustering (several seizures occurring close together in time) and the variations in brain responses to the same stimulation at different time points [8,37,41,61]. The results of the current study contribute to the open discussion regarding the origin of these fluctuations. In the following, we will first outline some basic concepts and positions in the discussion and then interpret the study's results in the context of those positions.

One of the interesting debates directly related to our study at the border between the seizure prediction and forecasting is whether the fluctuations in seizure susceptibility are due to "external" - not directly disease-related - fluctuations (e.g. sleep and wake cycle) or due to "internal" fluctuations in the seizure-related processes themselves (e.g. pathological chloride build-up due to epilepsy-related cell overactivity; e.g. Raimondo & Dulla, 2019), or both (superposition of the two). In the second scenario, where fluctuations in seizure susceptibility are driven by an "internal" epileptic process, seizure susceptibility would "spontaneously" increase in the epileptic brain (as opposed to a normal brain) until a critical level is reached and seizure is initiated, even in the absence of external stimuli/influences. At seizure termination, seizure susceptibility would be reset to a low level (from where it would then slowly start growing again). Related to this view is the "seizure begets seizure" theory [63,64], which highlights the disease-modifying effect of the seizure activity itself as well as the recurrent nature of seizure-like activity in *in vitro* animal models, where no external modulators are present. In favor of external modulators as drivers, on the other hand, are observations of sudden, seemingly random seizure initiation and the common alignment of seizure occurrence with sleep and wave cycles, as well as daily and hormonal cycles [42,44,65]. Considering the patient-specificity and other variations challenging the support in both directions, also an interplay of the two is a possible scenario, such that seizure-related fluctuations might be superimposed on external fluctuations or vice versa. An analogical example for such a superposition could be the occurrence of lightning during thunderstorms, where certain weather conditions ("*pro*-lightening" states) are necessary for enabling the lightning build-up-and-discharge mechanisms (including "*pre*-lightening" states).

Understanding the (potentially patient-specific) interplay of "external" and "internal" drivers, pro-ictal and pre-ictal states, and the different time scales involved - pre-ictal states are typically reported to occur minutes to hours before seizures, while pro-ictal states can last up to several days and months -, remains an open challenge.

In this study, we adopted an intermediate approach between the two worlds of seizure prediction and forecasting (the separation of which is, of course, oversimplified) in an effort to help disentangle the complex mechanisms involved in seizure generation. The chosen multi-day dataset of presurgical iEEG monitoring in epilepsy patients provided the means to compare the short-term (minutes before a seizure) and long-term (days before a seizure) time scales. While we found brain dynamic changes in the long-term, we did not find changes in the short-term. Importantly, in the studied dataset, "internal" seizure susceptibility mechanisms were manipulated by decreasing the administered drug dose [3]. Thus, a novelty of this study was to apply measures from seizure prediction in the context of a controlled progressive loss of seizure resilience [8] that should give rise to a pro-ictal state. We argue that the identified long-term differences are likely to reflect brain changes characteristic of pro-ictal states as opposed to pre-ictal states of individual seizure transitions. As in the case of pre-ictal states, an observed build-up should continue until seizure is reached. The missing short-term increase in this study could be an indication that the detected brain changes do, in fact, reflect a pro-ictal state.

Due to the chosen study set-up, as well as the fact that the observed brain changes were not linked with changes in the "external" factor day time assessed in the study, we further believe to have identified brain dynamics of "internal", directly disease-related pro-ictal states in the human brain. We did not find a significant correlation with linear time and drug dosage decrease (which we consider "internal" factors), even though previous accounts have linked anti-seizure medication effects and critical slowing and high-frequency changes [66]. We did, however, find a significant correlation of identified brain changes and the measured rate of spikes and HFOs. The function of spikes and HFOs in epilepsy remains an ongoing debate. While they could play a direct role in increasing seizure likelihood, they could also be a consequence of an increased seizure likelihood [28]. In both cases, however, they stand in a direct relationship to the ongoing epileptogenic processes, in line with their considered important role in epilepsy diagnosis [58]. Thus, we believe that they can be interpreted as an "internal" factor, supporting the relevance of our findings in the context of pro-ictal states in epilepsy.

Conclusion

This study highlights gamma oscillations and critical slowing as markers of pro-ictal, multi-day brain dynamics during the presurgical evaluation of epilepsy patients. While gamma power increased locally in the EZ, critical slowing increased network-wide across the different regions. Interestingly, the rate of spikes and HFOs, a hallmark of epilepsy, was consistently linked with the significant changes in brain dynamics identified in this study. Thus, gamma power and critical slowing could be useful tools to track epileptic brain states for the study of epilepsy mechanisms, or in the clinical setting, to track changes in seizure susceptibility during multi-day monitoring.

Acknowledgement:

This work was supported by the bilateral Barrande Mobility scheme, funded by the Ministry of Education, Youth and Sports of Czech Republic, project number MSMT–7125/2020-16 8J20FR037 and Campus France grant No. 44815QG, the Czech Science Foundation. project No. 21-32608S, by ERDF-Project Brain dynamics, No. CZ.02.01.01/00/22_008/0004643, and the long-term strategic development financing of the Institute of Computer Science (RVO:67985807) of the Czech Academy of Sciences.

Author Contribution:

IDZ, JK, AP, JC, EJB and JH conceived the study. JC, MD, JCS and LV are responsible for data collection and curation. IDZ, JK and AP analyzed the data under supervision of JH. IDZ and JK wrote the manuscript with contributions of AP, JC, EJB and JH. All co authors reviewed the manuscript.

Data Availability Statement:

Data available on request due to privacy/ethical restrictions.

Conflicts of Interest/Ethical Publication Statement:

None of the authors has any conflict of interest to disclose.

We confirm that we have read the Journal's position on issues involved in ethical publication and affirm that this report is consistent with those guidelines.

REFERENCES

1. Bartolomei F, Lagarde S, Wendling F, McGonigal A, Jirsa V, Guye M, et al. Defining epileptogenic networks: Contribution of SEEG and signal analysis. Epilepsia. 2017; 58(7):1131–47.

2. Paredes-Aragon E, AlKhaldi NA, Ballesteros-Herrera D, Mirsattari SM. Stereo-Encephalographic Presurgical Evaluation of Temporal Lobe Epilepsy: An Evolving Science. Front Neurol. 2022; 13:867458.

3. Hartl E, Seethaler M, Lauseker M, Rémi J, Vollmar C, Noachtar S. Impact of withdrawal of antiepileptic medication on the duration of focal onset seizures. Seizure. 2019; 67:40–4.

4. Friedman DE, Hirsch LJ. How Long Does It Take to Make an Accurate Diagnosis in an Epilepsy Monitoring Unit? J Clin Neurophysiol. 2009; 26(4):213–7.

5. Zhou Q, Hou X, Huang Z, Wang G. [Slow anti-epileptic drug taper protocol in video-EEG monitoring for presurgical evaluation of epilepsy]. Nan Fang Yi Ke Da Xue Xue Bao. 2012; 32(8):1197–200.

6. Jiruska P, Csicsvari J, Powell AD, Fox JE, Chang W-C, Vreugdenhil M, et al. High-Frequency Network Activity, Global Increase in Neuronal Activity, and Synchrony Expansion Precede Epileptic Seizures *In Vitro*. J Neurosci. 2010; 30(16):5690–701.

7. Mormann F, Andrzejak RG, Elger CE, Lehnertz K. Seizure prediction: the long and winding road. Brain. 2007; 130(2):314–33.

8. Chang W-C, Kudlacek J, Hlinka J, Chvojka J, Hadrava M, Kumpost V, et al. Loss of neuronal network resilience precedes seizures and determines the ictogenic nature of interictal synaptic perturbations. Nat Neurosci. 2018; 21(12):1742–52.

9. Dan B. Event forecasting in neurological disorders. Dev Med Child Neurol. 2022; 64(5):528–528.

10. Mormann F, Andrzejak RG. Seizure prediction: making mileage on the long and

winding road. Brain. 2016; 139(6):1625–7.

11. Usman SM, Khalid S, Akhtar R, Bortolotto Z, Bashir Z, Qiu H. Using scalp EEG and intracranial EEG signals for predicting epileptic seizures: Review of available methodologies. Seizure. 2019; 71:258–69.

12. Freestone DR, Karoly PJ, Peterson ADH, Kuhlmann L, Lai A, Goodarzy F, et al. Seizure Prediction: Science Fiction or Soon to Become Reality? Curr Neurol Neurosci Rep. 2015; 15(11):73.

13. Hussein R, Ward R. Quantitative and Qualitative Analyses of Invasive EEG for Epileptic Seizure Prediction. Austin J Clin Neurol [Internet]. 2021 [cited 2023]; 8(1). Available from: http://austinpublishinggroup.com/clinical-neurology/fulltext/ajcn-v8-id1144.php

14. Maturana MI, Meisel C, Dell K, Karoly PJ, D'Souza W, Grayden DB, et al. Critical slowing down as a biomarker for seizure susceptibility. Nat Commun. 2020; 11(1):2172.

15. Jacobs J. High-Frequency Oscillations (HFO). In: Invasive Studies of the Human Epileptic Brain [Internet]. Oxford University Press; 2018 [cited 2023]. p. 131–48. Available from: https://academic.oup.com/book/24511/chapter/187641196

16. Jacobs J, Zelmann R, Jirsch J, Chander R, Dubeau C-ÉCF, Gotman J. High frequency oscillations (80-500 Hz) in the preictal period in patients with focal seizures. Epilepsia. 2009; 50(7):1780–92.

17. Malinowska U, Bergey GK, Harezlak J, Jouny CC. Identification of seizure onset zone and preictal state based on characteristics of high frequency oscillations. Clin Neurophysiol. 2015; 126(8):1505–13.

18. Scott JM, Ren S, Gliske SV, Stacey WC. Preictal variability of high-frequency oscillation rates in refractory epilepsy. Epilepsia. 2020; 61(11):2521–33.

19. Hughes JR. Gamma, fast, and ultrafast waves of the brain: Their relationships with epilepsy and behavior. Epilepsy Behav. 2008; 13(1):25–31.

20. Medvedev AV, Murro AM, Meador KJ. Abnormal interictal gamma activity may manifest a seizure onset zone in temporal lobe epilepsy. Int J Neural Syst. 2011; 21(02):103–14.

21. Janca R, Jahodova A, Hlinka J, Jezdik P, Svobodova L, Kudr M, et al. Ictal gamma-band interactions localize ictogenic nodes of the epileptic network in focal cortical dysplasia. Clin Neurophysiol Off J Int Fed Clin Neurophysiol. 2021; 132(8):1927–36.

22. Mormann F, Lehnertz K, David P, E. Elger C. Mean phase coherence as a measure for phase synchronization and its application to the EEG of epilepsy patients. Phys Nonlinear Phenom. 2000; 144(3–4):358–69.

23. Weiss SA, Lemesiou A, Connors R, Banks GP, McKhann GM, Goodman RR, et al. Seizure localization using ictal phase-locked high gamma: A retrospective surgical outcome study. Neurology. 2015; 84(23):2320–8.

24. Zweiphenning WJEM, Keijzer HM, Diessen E, Van 'T Klooster MA, Klink NEC, Leijten FSS, et al. Increased gamma and decreased fast ripple connections of epileptic tissue: A high-frequency directed network approach. Epilepsia. 2019; 60(9):1908–20.

25. Sumsky S, Greenfield LJ. Network analysis of preictal iEEG reveals changes in network structure preceding seizure onset. Sci Rep. 2022; 12(1):12526.

26. Naftulin JS, Ahmed OJ, Piantoni G, Eichenlaub J-B, Martinet L-E, Kramer MA, et al. Ictal and preictal power changes outside of the seizure focus correlate with seizure generalization. Epilepsia. 2018; 59(7):1398–409.

27. Schulze-Bonhage A. Seizure prediction: Time for new, multimodal and ultra-long-term approaches. Clin Neurophysiol. 2022; 133:152–3.

28. Baud MO, Proix T, Rao VR, Schindler K. Chance and risk in epilepsy. Curr Opin Neurol. 2020; 33(2):163–72.

29. Baud MO, Kleen JK, Mirro EA, Andrechak JC, King-Stephens D, Chang EF, et al. Multi-day rhythms modulate seizure risk in epilepsy. Nat Commun. 2018; 9(1):88.

30. Cook MJ, O'Brien TJ, Berkovic SF, Murphy M, Morokoff A, Fabinyi G, et al. Prediction of seizure likelihood with a long-term, implanted seizure advisory system in patients with drug-resistant epilepsy: a first-in-man study. Lancet Neurol. 2013; 12(6):563–71.

31. Freestone DR, Karoly PJ, Peterson ADH, Kuhlmann L, Lai A, Goodarzy F, et al. Seizure Prediction: Science Fiction or Soon to Become Reality? Curr Neurol Neurosci Rep. 2015; 15(11):73.

32. Karoly PJ, Goldenholz DM, Freestone DR, Moss RE, Grayden DB, Theodore WH, et al. Circadian and circaseptan rhythms in human epilepsy: a retrospective cohort study. Lancet Neurol. 2018; 17(11):977–85.

33. Proix T, Truccolo W, Leguia MG, Tcheng TK, King-Stephens D, Rao VR, et al. Forecasting seizure risk in adults with focal epilepsy: a development and validation study. Lancet Neurol. 2021; 20(2):127–35.

34. Stirling RE, Cook MJ, Grayden DB, Karoly PJ. Seizure forecasting and cyclic control of seizures. Epilepsia [Internet]. 2021 [cited 2022]; 62(S1). Available from: https://onlinelibrary.wiley.com/doi/10.1111/epi.16541

35. Kudlacek J, Chvojka J, Kumpost V, Hermanovska B, Posusta A, Jefferys JGR, et al. Long-term seizure dynamics are determined by the nature of seizures and the mutual interactions between them. Neurobiol Dis. 2021; 154:105347.

36. Pérez-Cervera A, Hlinka J. Perturbations both trigger and delay seizures due to generic properties of slow-fast relaxation oscillators. Taylor PN, editor. PLOS Comput Biol. 2021; 17(3):e1008521.

37. Jiruska P, Powell AD, Deans JK, Jefferys JGR. Effects of direct brain stimulation depend on seizure dynamics. Epilepsia. 2010; 51(s3):93–7.

38. Chang W-C, Kudlacek J, Hlinka J, Chvojka J, Hadrava M, Kumpost V, et al. Loss of neuronal network resilience precedes seizures and determines the ictogenic nature of interictal synaptic perturbations. Nat Neurosci. 2018; 21(12):1742–52.

39. Panagiotopoulou M, Papasavvas CA, Schroeder GM, Thomas RH, Taylor PN, Wang Y. Fluctuations in EEG band power at subject-specific timescales over minutes to days explain changes in seizure evolutions. Hum Brain Mapp. 2022; 43(8):2460–77.

40. Schroeder GM, Diehl B, Chowdhury FA, Duncan JS, de Tisi J, Trevelyan AJ, et al. Seizure pathways change on circadian and slower timescales in individual patients with focal epilepsy. Proc Natl Acad Sci. 2020; 117(20):11048–58.

41. Kudlacek J, Chvojka J, Kumpost V, Hermanovska B, Posusta A, Jefferys JGR, et al. Long-term seizure dynamics are determined by the nature of seizures and the mutual interactions between them. Neurobiol Dis. 2021; 154:105347.

42. Bernard C, Frauscher B, Gelinas J, Timofeev I. Sleep, oscillations, and epilepsy.

Epilepsia. 2023; :epi.17664.

43. Karoly PJ, Goldenholz DM, Freestone DR, Moss RE, Grayden DB, Theodore WH, et al. Circadian and circaseptan rhythms in human epilepsy: a retrospective cohort study. Lancet Neurol. 2018; 17(11):977–85.

44. Payne DE, Dell KL, Karoly PJ, Kremen V, Gerla V, Kuhlmann L, et al. Identifying seizure risk factors: A comparison of sleep, weather, and temporal features using a Bayesian forecast. Epilepsia. 2021; 62(2):371–82.

45. Meisel C. Antiepileptic drugs induce subcritical dynamics in human cortical networks. Proc Natl Acad Sci. 2020; 117(20):11118–25.

46. Meisel C, Schulze-Bonhage A, Freestone D, Cook MJ, Achermann P, Plenz D. Intrinsic excitability measures track antiepileptic drug action and uncover increasing/decreasing excitability over the wake/sleep cycle. Proc Natl Acad Sci. 2015; 112(47):14694–9.

47. Bruña R, Maestú F, Pereda E. Phase locking value revisited: teaching new tricks to an old dog. J Neural Eng. 2018; 15(5):056011.

48. Roehri N, Pizzo F, Lagarde S, Lambert I, Nica A, McGonigal A, et al. High-frequency oscillations are not better biomarkers of epileptogenic tissues than spikes. Ann Neurol. 2018; 83(1):84–97.

49. Wieser HG, Blume WT, Fish D, Goldensohn E, Hufnagel A, King D, et al. Proposal for a New Classification of Outcome with Respect to Epileptic Seizures Following Epilepsy Surgery. Epilepsia. 2001; 42(s2):282–6.

50. Delorme A, Makeig S. EEGLAB: an open source toolbox for analysis of single-trial EEG dynamics including independent component analysis. J Neurosci Methods. 2004; 134(1):9–21.

51. Lachaux J-P, Rodriguez E, Martinerie J, Varela FJ. Measuring phase synchrony in brain signals. Hum Brain Mapp. 1999; 8(4):194–208.

52. Baud MO, Kleen JK, Mirro EA, Andrechak JC, King-Stephens D, Chang EF, et al. Multi-day rhythms modulate seizure risk in epilepsy. Nat Commun. 2018; 9(1):88.

53. Roehri N, Lina J-M, Mosher JC, Bartolomei F, Benar C-G. Time-Frequency Strategies for Increasing High-Frequency Oscillation Detectability in Intracerebral

EEG. IEEE Trans Biomed Eng. 2016; 63(12):2595–606.

54. Colombet B, Woodman M, Badier JM, Bénar CG. AnyWave: A cross-platform and modular software for visualizing and processing electrophysiological signals. J Neurosci Methods. 2015; 242:118–26.

55. Chang S, Wang J, Liu C, Yi G, Lu M, Che Y, et al. A Data Driven Experimental System for Individualized Brain Stimulation Design and Validation. IEEE Trans Neural Syst Rehabil Eng. 2021; 29:1848–57.

56. Panagiotopoulou M, Papasavvas CA, Schroeder GM, Thomas RH, Taylor PN, Wang Y. Fluctuations in EEG band power at subject-specific timescales over minutes to days explain changes in seizure evolutions. Hum Brain Mapp. 2022; 43(8):2460–77.

57. Maturana MI, Meisel C, Dell K, Karoly PJ, D'Souza W, Grayden DB, et al. Critical slowing down as a biomarker for seizure susceptibility. Nat Commun. 2020; 11(1):2172.

58. Zijlmans M, Zweiphenning W, van Klink N. Changing concepts in presurgical assessment for epilepsy surgery. Nat Rev Neurol. 2019; 15(10):594–606.

59. Scott JM, Gliske SV, Kuhlmann L, Stacey WC. Viability of Preictal High-Frequency Oscillation Rates as a Biomarker for Seizure Prediction. Front Hum Neurosci. 2021; 14:612899.

60. Jmail N, Gavaret M, Bartolomei F, Bénar C-G. Despiking SEEG signals reveals dynamics of gamma band preictal activity. Physiol Meas. 2017; 38(2):N42–56.

61. Pérez-Cervera A, Hlinka J. Perturbations both trigger and delay seizures due to generic properties of slow-fast relaxation oscillators. Taylor PN, editor. PLOS Comput Biol. 2021; 17(3):e1008521.

62. Raimondo JV, Dulla C. When a Good Cop Turns Bad: The Pro-Ictal Action of Parvalbumin Expressing Interneurons During Seizures. Epilepsy Curr. 2019; 19(4):256–7.

63. Gowers WR. Epilepsy and Other Chronic Convulsive Diseases: Their Causes, Symptoms, & Treatment [Internet]. J. & A. Churchill; 1881. Available from: https://books.google.cz/books?id = URoDAAAAQAAJ

64. Jiruska P, Freestone D, Gnatkovsky V, Wang Y. An update on the seizures beget

seizures theory. Epilepsia. 2023; :epi.17721.

65. Mitsis GD, Anastasiadou MN, Christodoulakis M, Papathanasiou ES, Papacostas SS, Hadjipapas A. Functional brain networks of patients with epilepsy exhibit pronounced multiscale periodicities, which correlate with seizure onset. Hum Brain Mapp. 2020; 41(8):2059–76.

66. Duncan JS. Antiepileptic Drugs and the Electroencephalogram. Epilepsia. 1987; 28(3):259–66.

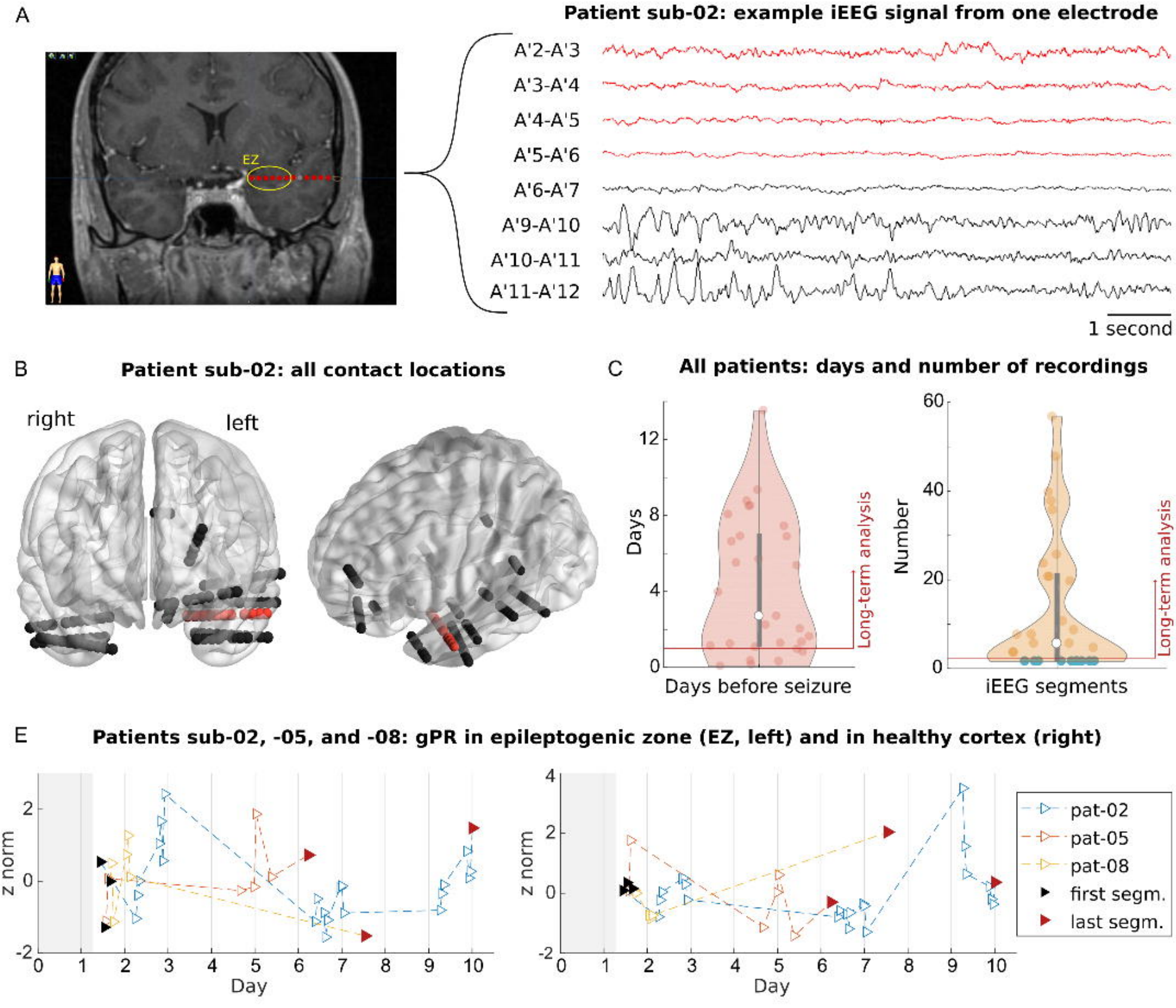
A
Patient sub-02: example iEEG signal from one electrode
EZ
A'2-A'3
A'3-A'4
A'4-A'5
A'5-A'6
A'6-A'7
A'9-A'10
A'10-A'11
A'11-A'12
1 second
B
Patient sub-02: all contact locations
right
left
C
All patients: days and number of recordings
Days
Days before seizure
Long-term analysis
Number
iEEG segments
Long-term analysis
E
Patients sub-02, -05, and -08: gPR in epileptogenic zone (EZ, left) and in healthy cortex (right)
z norm
Day
z norm
Day
pat-02
pat-05
pat-08
first segm.
last segm.

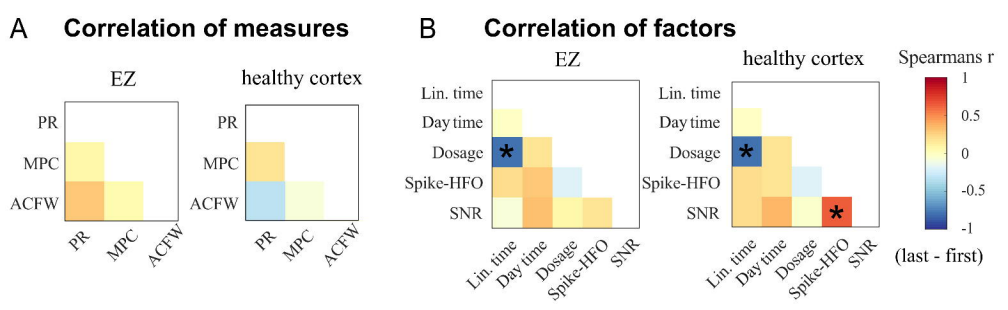
A
Correlation of measures
EZ
healthy cortex
PR
MPC
ACFW
PR
MPC
ACFW
B
Correlation of factors
EZ
healthy cortex
Spearmans r
1
0.5
0
-0.5
-1
(last - first)
Lin. time
Day time
Dosage
Spike-HFO
SNR
*
*
*

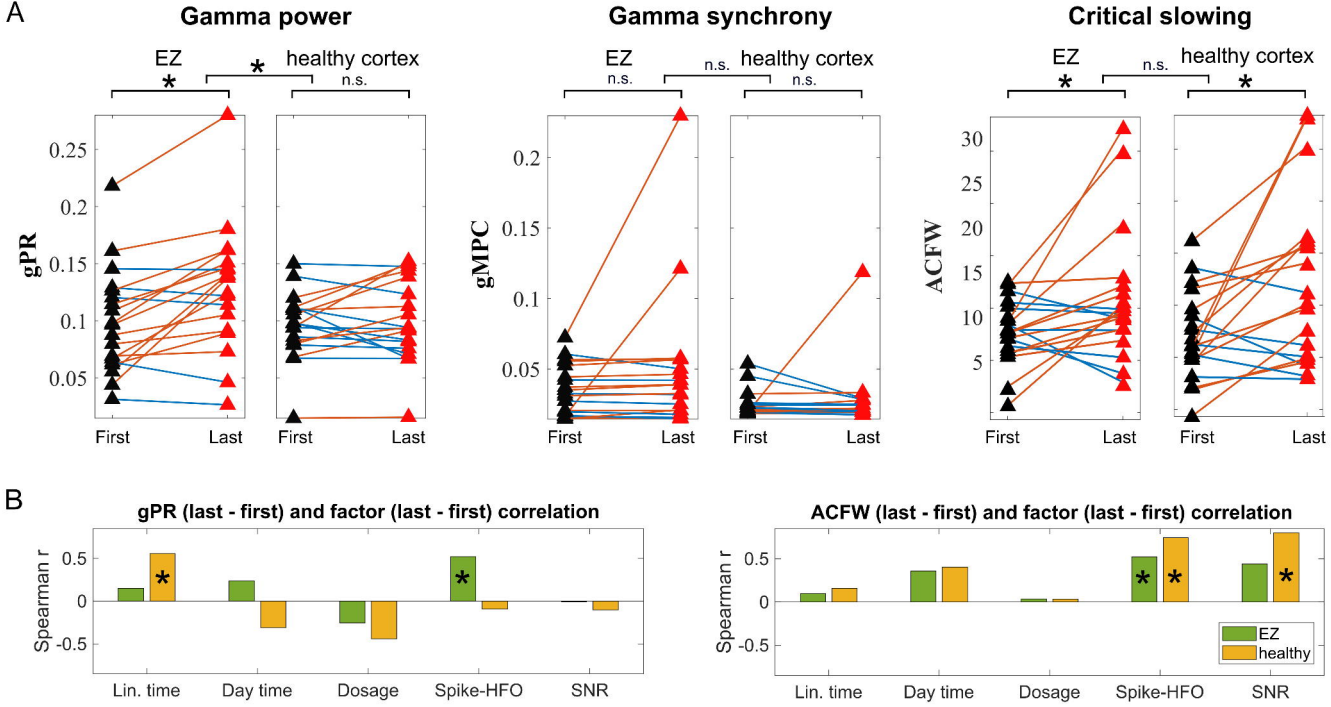
A
Gamma power
EZ
healthy cortex
*
*
n.s.
gPR
0.25
0.2
0.15
0.1
0.05
First
Last
First
Last
Gamma synchrony
EZ
healthy cortex
n.s.
n.s.
n.s.
gMPC
0.2
0.15
0.1
0.05
First
Last
First
Last
Critical slowing
EZ
healthy cortex
*
n.s.
*
ACFW
30
25
20
15
10
5
First
Last
First
Last
B
gPR (last - first) and factor (last - first) correlation
Spearman r
0.5
0
-0.5
*
*
Lin. time
Day time
Dosage
Spike-HFO
SNR
ACFW (last - first) and factor (last - first) correlation
Spearman r
0.5
0
-0.5
*
*
*
EZ
healthy
Lin. time
Day time
Dosage
Spike-HFO
SNR

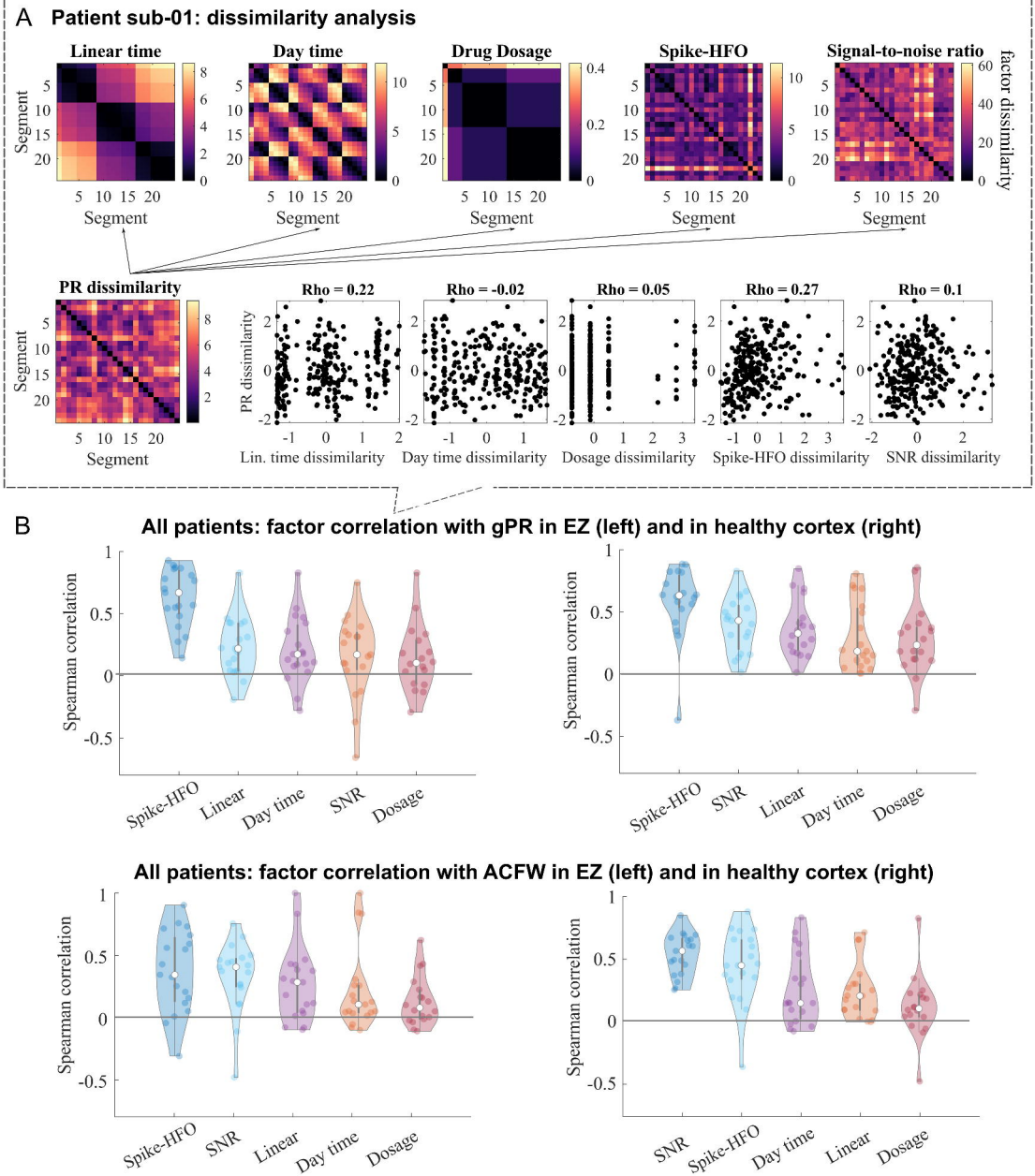
A
Patient sub-01: dissimilarity analysis
Linear time
Day time
Drug Dosage
Spike-HFO
Signal-to-noise ratio
factor dissimilarity
Segment
PR dissimilarity
Rho = 0.22
Rho = -0.02
Rho = 0.05
Rho = 0.27
Rho = 0.1
PR dissimilarity
Lin. time dissimilarity
Day time dissimilarity
Dosage dissimilarity
Spike-HFO dissimilarity
SNR dissimilarity
B
All patients: factor correlation with gPR in EZ (left) and in healthy cortex (right)
Spearman correlation
Spike-HFO
Linear
Day time
SNR
Dosage
All patients: factor correlation with ACFW in EZ (left) and in healthy cortex (right)

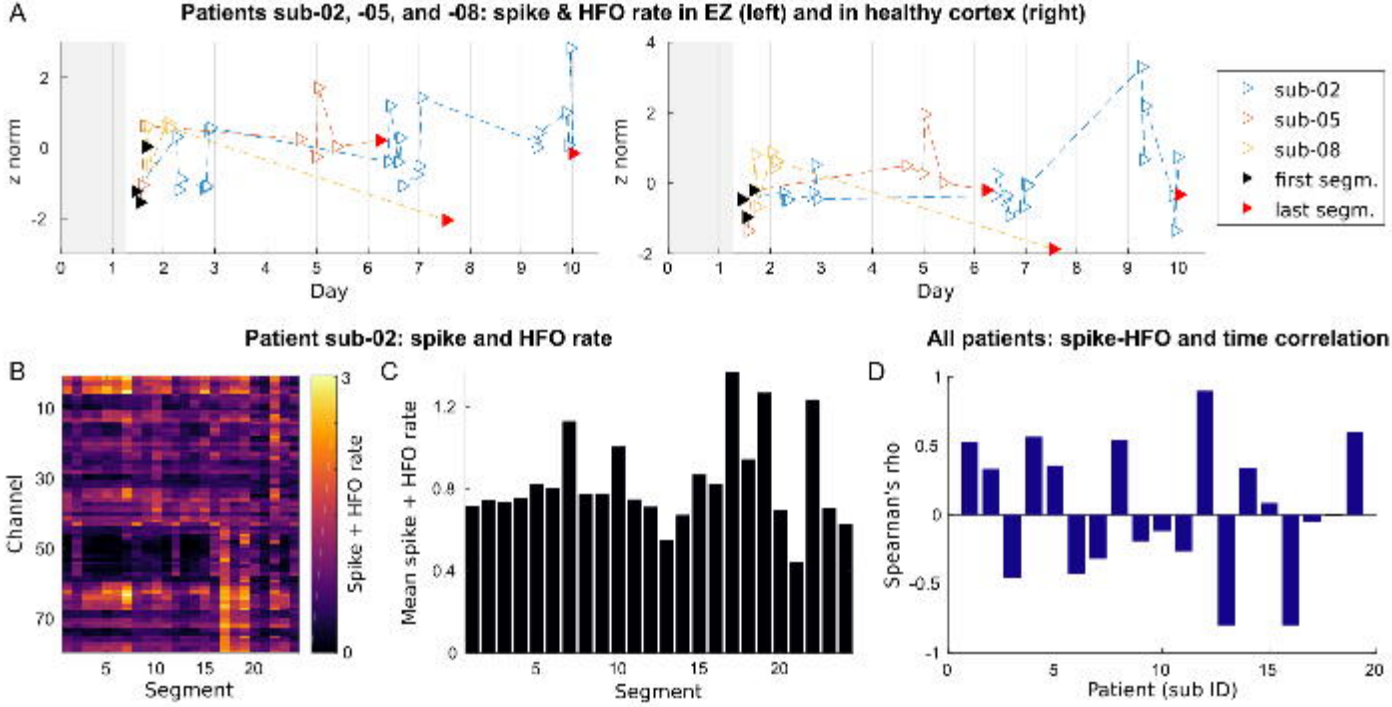
A
Patients sub-02, -05, and -08: spike & HFO rate in EZ (left) and in healthy cortex (right)
z norm
Day
sub-02
sub-05
sub-08
first segm.
last segm.
B
Patient sub-02: spike and HFO rate
Channel
Segment
Spike + HFO rate
C
Mean spike + HFO rate
Segment
D
All patients: spike-HFO and time correlation
Spearman's rho
Patient (sub ID)

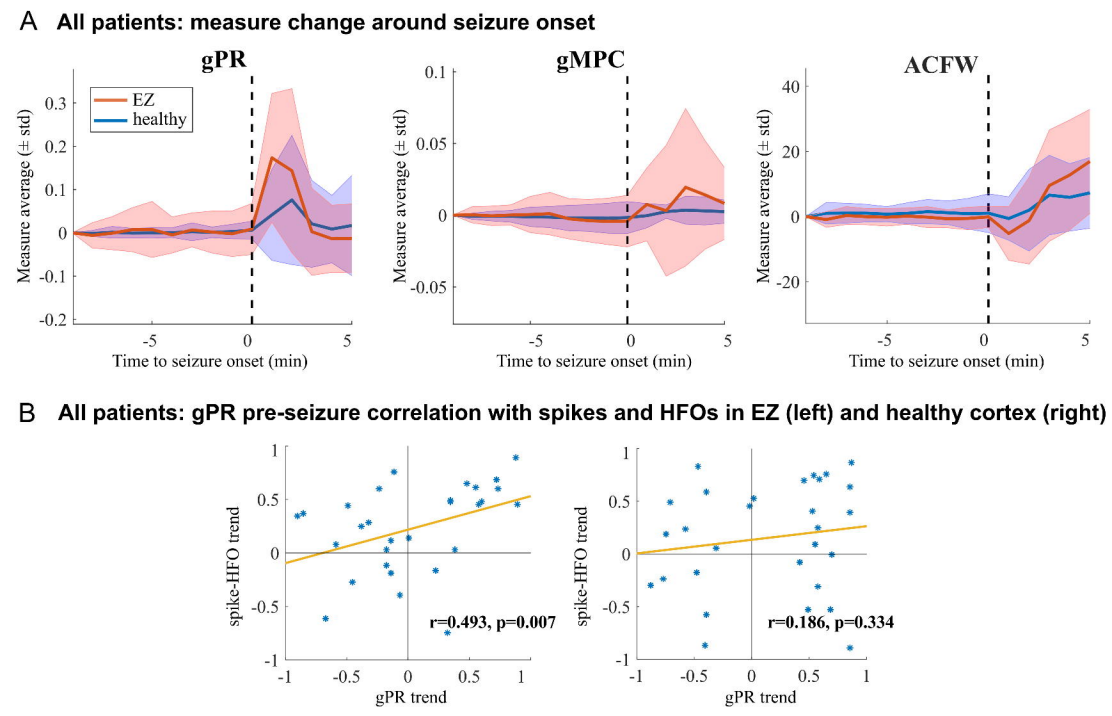
A All patients: measure change around seizure onset
gPR
gMPC
ACFW
EZ
healthy
Measure average (± std)
Time to seizure onset (min)
B All patients: gPR pre-seizure correlation with spikes and HFOs in EZ (left) and healthy cortex (right)
spike-HFO trend
gPR trend
r=0.493, p=0.007
r=0.186, p=0.334

Patient	MRI lesion(s)	EZ localization*	duration**	sex	electrodes	channels***	channels EZ	outcome****
sub-01	R HS	R temporal	7	M	16	126	22	ILAE 1 (2y)
sub-02	R HS	L amygdala & hippocampus	6	M	12	117	11	ILAE 4 (2y)
sub-03	R HS	R temporal	21	F	14	124	5	ILAE 1 (2y)
sub-04	R HS, sequelae of ganglioma surgery	R temporal	11	F	11	125	12	ILAE 1 (1y)
sub-05	none[a]	L temporal	6	M	11	118	16	ILAE 5 (11y)
sub-06	R HS	R temporopolar	16	M	11	111	35	ILAE 5 (12y)
sub-08	R HS	R temporal	5	M	11	120	6	ILAE 1 (3y)
sub-09	HS	L temporal	38	M	12	88	8	ILAE 3 (3y)
sub-10	bilateral HS	L temporal	19	M	10	117	11	NA
sub-12	L HS	L temporal	10	M	10	117	10	ILAE 1 (4y)
sub-15	L colliculus cyst, L mamillar and fornix atrophy	L frontal	18	M	14	127	2	NA
sub-16	L reactional gliosis, ischemic neuronal lesions	L temporal	32	F	11	114	2	ILAE 5 (9y)
sub-17	R cortical temporal atrophy	bitemporal	50	F	12	120	15	NA
sub-18	bilateral post traumatic sequelae	bitemporal	8	M	13	125	5	NA
sub-20	L HS	L temporal	20	M	13	126	12	ILAE 4 (6y)
sub-21	L temporopolar meningoencephalocelis	L temporal	20	M	12	127	61	NA
sub-22	none	L temporal & L medial	13	M	14	127	4	NA
sub-23	L HS, occipito-temporo-parietal sequelae	L temporal	29	M	10	111	2	NA
sub-24	L HS	L temporal	14	F	11	118	3	ILAE 1 (6y)
sub-25	L HS	L temporal	10	F	13	127	10	ILAE 1 (4y)
sub-26	R HS	R temporal	17	M	9	127	4	ILAE 1 (4y)
sub-27	R HS	R temporal & R orbitofrontal	49	F	12	112	17	NA
sub-28	L HS	L temporal	13	M	11	119	12	ILAE 4 (7y)
sub-30	R HS	R temporal	8	F	7	83	14	ILAE 1 (8y)
sub-31	R hippocampal atrophy, medotemporal & polar hypersignal[b]	L temporal	9	M	13	120	9	NA
sub-32	L cortical frontotemporal atrophy	L insular	25	F	9	83	20	ILAE 1 (4y)
sub-33	sequelae of surgery of plexus choroid carcinoma	R temporal	17	F	9	97	9	ILAE 1 (5y)
sub-34	L hippocampal heterotopia	bitemporal	34	M	14	127	24	NA
sub-35	DNET	R temporal	4	M	11	120	9	ILAE 1 (8y)

*EZ localization after the final medical conclusions at the end of the SEEG; **duration of epilepsy at time of hospitalization; ***channel numbers as available in data recording files; ****surgery outcome – if offered – as assessed at a variable time interval after presurgical evaluation, denoted for each patient in years (y).

[a]reactional gliosis, ischemic neuronal lesions; [b]"neuronal injury associated with neuronal dispersion", ischemic neuronal lesion in amygdala, gliosis in lateral temporal

DNET: Dysembryoplastic Neuroepithelial Tumor; F: female; HS: hippocampal sclerosis; ILAE: International League Against Epilepsy; M: male; MRI: magnetic resonance imaging; NA: not administered